



Particle fluxes in submarine canyons along a sediment-starved continental margin and in the adjacent open slope and basin in the SW Mediterranean Sea

Marta Tarrés^a, Marc Cerdà-Domènech^a, Rut Pedrosa-Pàmies^{a,b}, Aitor Rumín-Caparrós^a, Antoni Calafat^a, Miquel Canals^a, Anna Sanchez-Vidal^{a,*}

^a GRC Geociències Marines, Dept. Dinàmica de la Terra i de l'Oceà, Facultat de Ciències de la Terra, Universitat de Barcelona, 08028 Barcelona, Spain

^b The Ecosystems Center, Marine Biological Laboratory, Woods Hole, MA, USA

ARTICLE INFO

Keywords:

Particle fluxes
Sediment-starved continental margin
Submarine canyons
Open slope
Deep basin
Mediterranean Sea

ABSTRACT

Investigating the transfer of particulate matter from the continental shelf to the deep basin is critical to understand the functioning of deep sea ecosystems. In this paper we present novel results on the temporal variability of particle fluxes to the deep in three physiographic domains of a 240 km long margin segment and nearby basin off Murcia and Almeria provinces in the SW Mediterranean Sea, which are submarine canyons forming a rather diverse set (namely Escombreras, Garrucha-Almanzora and Almeria), the adjacent open slope and the deep basin.

This margin is located off one of the driest regions in Europe and, therefore, its study may help understanding how mainland aridity translates into the export of particles to deep margin environments. Five mooring lines equipped with currentmeters, turbidity-meters and sediment traps were deployed for one entire annual cycle, from March 2015 to March 2016. We combine oceanographic, hydrological and meteorological data with grain size and bulk elemental data (organic carbon, opal, CaCO₃, lithogenic) from the collected sinking particles to understand what drives particle transfers in such an under-studied setting, and to quantify the resulting fluxes and assess their spatio-temporal variability.

Weighted total mass fluxes in canyons range from 1.64 g m⁻² d⁻¹ in Almeria Canyon to 7.33 g m⁻² d⁻¹ in Garrucha-Almanzora Canyon system, which are rather low values compared to other submarine canyons in the Western Mediterranean Sea. This results from the absence of extreme wind-storm events during the investigated time period combined with the reduced sediment input to the inner shelf by river systems in the study area. Our results also show that wind-storms are the main trigger for off-shelf particle transport to the deep margin, both within submarine canyons and over the open slope. The most significant transfer period is associated to a set of north-eastern storms in early spring 2015, when the off-shelf transport likely was promoted by storm-induced downwelling. However, the prevailing oceanographic conditions restricts the advection of water down the canyon heads to a few hundred meters, thus promoting a bottom-detached transport of particles seaward. Overall physiography, canyon head incision into the continental shelf and the distance of the canyon head to the shoreline (e.g. very short in Garrucha Canyon) play a key role in particle trapping capability and, therefore, in easing downslope particle transport. Further, bottom trawling activities around the Garrucha-Almanzora Canyon system, feed a nepheloid layer at depths in excess of 400 m, subsequently enhancing particle fluxes throughout the study period. In contrast, maximum particle fluxes in the deep basin respond to seasonal phytoplankton blooms.

Our study shows that particle export from the shallow inner margin to the deep outer margin in sediment-starved settings, even if limited, does occur as dominated by atmosphere and ocean driven short-lived events. However, that export does not reach too far as at several tens of kilometres from the shelf edge advective fluxes are replaced by vertical ones impelled by phytoplankton dynamics.

* Corresponding author.

E-mail address: anna.sanchez@ub.edu (A. Sanchez-Vidal).

1. Introduction

Continental margins are the areas that connect the continent and the deep sea. These areas are where most of the sediments are deposited, and are an important source of material to deep sea ecosystems. Materials supplied by the rivers (and autochthonous biological production) are transferred from the continental shelf to the slope and deep basin, especially in those areas incised by submarine canyons. Submarine canyons are large geomorphic features carved on continental margins that act as preferential conduits for particulate matter export from the continental shelf to the deep margin and basin (Drake and Gorsline, 1973; Shepard et al., 1979; Xu et al., 2004; Heussner et al., 2006; Canals et al., 2006; Puig et al., 2014). Canyons are key features for the transfer and sinking, which are often episodic, of organic carbon (OC) and nutrients (Pasqual et al., 2010; Kiriakoulakis et al., 2011; Sanchez-Vidal et al., 2012; Pedrosa-Pàmies et al., 2013), while also facilitating the delivery of litter and chemical pollutants to deep ecosystems (Palanques et al., 2008a; Ramirez-Llodra et al., 2013; Dumas et al., 2014; Tubau et al., 2015).

To date, studies on particle fluxes within submarine canyons around the Iberian Peninsula margins have focused on specific segments such as the North Catalan and Gulf of Lion margins (Heussner et al., 2006; Martín et al., 2006; Durrieu de Madron et al., 2008; Pasqual et al., 2010; Sanchez-Vidal et al., 2012; Canals et al., 2013 and references therein), the Portuguese margin (Schmidt et al., 2001; de Stigter et al., 2007, 2011; Martín et al., 2011), margins of the Western Alboran Sea (Puig et al., 2004; Palanques et al., 2005) and the Cantabrian margin and neighbouring areas (Heussner et al., 1999; Schmidt et al., 2014; Romero-Romero et al., 2016; Rumin-Caparrós et al., 2016). These studies illustrate the markedly different behaviour between submarine canyons in the micro-tidal Western Mediterranean Sea and those in the meso-tidal Atlantic Ocean, where high swells are common. Compared to other canyons in the Western Mediterranean Sea and, more generally off Iberia and nearby areas, the sedimentary dynamics of submarine canyons off south-eastern Spain have been barely investigated (Puig et al., 2017), particularly because of two main reasons: (i) low river discharge resulting in reduced sediment supply to the continental margin; and (ii) lack of high-energy processes other than storms, such as those occurring in other areas, which have subsequently attracted the researchers' interest (e.g. dense shelf water cascading, DSWC, in the NW Mediterranean Sea—see further down—; Canals et al., 2006).

Submarine canyons from the Western Mediterranean Sea exhibit sediment transport interannual variability, reflecting complex interaction between the diverse forcing factors (atmospheric, hydrologic and oceanographic conditions) (Heussner et al., 2006; Palanques et al., 2006a, 2008b; Ogston et al., 2008). It has been documented in the NW Mediterranean region that during major storms sediments deposited on the continental shelf and canyon heads can be remobilized and flushed down-canyon (Canals et al., 2006; Palanques et al., 2006a; Sanchez-Vidal et al., 2012; Pedrosa-Pàmies et al., 2013), triggering large sediment export to the deep margin and basin (Sanchez-Vidal et al., 2012; Puig et al., 2014). Storm-induced downwelling there contributes to the off-shelf transfer of particulate matter, forced by a strong cyclonic circulation and along the coast water convergence during eastern storms (Ulses et al., 2008; Palanques et al., 2008b; Martín et al., 2013). Another highly relevant process occurring in the NW Mediterranean Sea is DSWC following formation of dense water over the continental shelf and subsequent near-bottom, gravity-driven sinking due to loss of buoyancy. Dense shelf water forms mostly in the Gulf of Lion during favourable winters, characterised by persistent cold and dry northern winds (Durrieu de Madron et al., 2008; Canals et al., 2013). Both dense shelf water formation and cascading present a high degree of interannual variability (Béthoux et al., 2002; Durrieu de Madron et al., 2005). Submarine canyons in the area behave as main conduits for particle-laden cascading waters, which in the absence of submarine canyons can flow downslope anyway until reaching their neutral buoyancy depth (Canals et al.,

2006). DSWC occurs in the form of short-lived metoceanographic events deeply impacting the deep ecosystem and associated benthic fauna by supplying large amounts of organic carbon (OC) (Company et al., 2008; Pusceddu et al., 2013). The amount and quality of the sinking particles is modulated by the occurrence of river floods and autochthonous biological production (Guillén et al., 2006; Fabres et al., 2008; Sanchez-Vidal et al., 2013; Lopez-Fernandez et al., 2013a).

Anthropogenic activities also impact the sediment dynamics of submarine canyons. Bottom trawling gear in particular erodes canyon upper flanks (Puig et al., 2012; Martín et al., 2014a), resulting in the remobilization of sediments that are channelized by tributaries (Martín et al., 2014b), ultimately increasing sediment accumulation rates in canyon axes (Paradis et al., 2017).

The non-occurrence of DSWC and the micro-tidal regime in the SW Mediterranean Sea raise the question about the relevance of sediment transfers to the deep margin and basin in this area, while also pointing to the need to quantify the overall fluxes and their composition, including organic matter (OM) contents, to determine possible relationships with specific forcing conditions, and to establish the periodicity of transfer events. These questions become more noteworthy when considering the lack of discharge from river systems during most of the year, severely limiting to rare time periods the supply of terrestrial sediments to the margin (Liquete et al., 2005).

This study focuses on the temporal variability of near-bottom and mid-water particle fluxes and associated oceanographic parameters over one-year in the mid-course of three submarine canyons (Escombreras, Garrucha-Almanzora and Almeria), in the open slope north of Garrucha-Almanzora Canyon, and in the deep basin in the Gulf of Vera, as investigated by means of sediment traps and currentmeters deployed in situ. The aim of the present study is to fill a gap in the knowledge of shelf-to-deep basin mass transfer in the SW Mediterranean Sea and, more generally, in sediment-starved margin segments. The simultaneous study of these three environments (canyons, open slope and deep basin) is also needed to better understand eventual interconnections amongst them.

2. Overall setting

The study area encompasses the Gulf of Vera to the north and the Gulf of Almeria to the south, in the SW Mediterranean Sea (Fig. 1). Climate is semi-arid, with low mean annual rainfall (<500 mm yr⁻¹) (AEMET, 2011). In spite of low annual precipitation, involving dry or almost dry streams during most of the year, fast flooding events occur in the region mainly in autumn months (Machado et al., 2011). The main rivers in the area are, in a clockwise direction, Almanzora, Antas, Aguas and Andarax (Fig. 1). Almanzora River is the main hydrological system, with a watershed of 2,611 km² (Puig et al., 2017), followed by the Andarax River system with 2,160.5 km² (Liquete et al., 2005). Both rivers feed delta and prodelta systems (Sanz et al., 2002; Liquete et al., 2005).

Wind regime in the study area is dominated by NE to SW flux in Cape of Palos and ENE to WSW in Cape of Gata, which may trigger significant wave heights (H_s) of < 5 m with wave periods of 6–7 s (Puig et al., 2017). Less frequent, stronger inter-annual wind events are able to generate 5 m < H_s < 7 m, generally during autumn and winter months. Events triggering major storms with waves between 5 m $\leq H_s < 6$ m can occur every 2–3 years, whereas for storms with waves with H_s equal or above 6 m the return period is longer than 13 years (<https://www.puertos.es>).

Prevailing surface circulation in the Gulf of Vera is southwards to Cape of Gata. In the neighbouring Alboran Sea the inflow of the Atlantic jet through the Gibraltar Strait forms two main non-permanent anticyclonic gyres, known as the western and eastern Alboran gyres (WAG and EAG, respectively). The encounter of the Mediterranean water from the north and west with the less saline Atlantic Water coming from the Alboran Sea produces a strong baroclinic jet, called Almeria-Oran Front (AOF), which extends in a NW-SE direction from Spanish to Algerian

coasts (Tintore et al., 1988). The semi-permanent AOF represents the eastern limit of the Alboran Sea circulation system and is controlled at its eastern edge by the geographic position and strength of the EAG, which usually forms during summer-autumn (Vargas-Yáñez et al., 2002; Renault et al., 2012). Intermediate and deep Mediterranean waters circulate towards the Strait of Gibraltar following the Spanish continental margin (Millot, 1999). Phytoplankton blooms in the study area usually extend from November to March (García-Gorrioz and Carr, 2001).

The study area comprises three margin segments, which are the Mazarron and Palomares margins within the Gulf of Vera, with E-W and NE-SW general orientation, respectively, and the Almeria margin south and west of Cape of Gata (Fig. 1). Neogene and Quaternary tectonics have determined the evolution and morphology of these margins (Estrada et al., 1997; Comas et al., 1999; Acosta et al., 2013). Most submarine canyons in the area follow fault systems, some of which are active, as is the case for the Almeria (ALC) and Escombreras (ESC) canyons (Estrada et al., 1997; Gràcia et al., 2006; Acosta et al., 2013; Pérez-Hernández et al., 2014). However, it is uncertain if the faults guiding Alias-Almanzora (AL-ALMC) and Gata (GT) canyon systems (Fig. 1) are still active (Gómez de la Peña et al., 2016).

The study area presents a narrow continental shelf (Lobo et al., 2014), which in the Mazarron margin ranges from 13 km to the east to < 4 km to the west, to then open to a steep continental slope dominated by multiple short canyons from ~200 m depth downwards (Acosta et al., 2013). The Palomares shelf generally is < 11 km wide (Pérez-Hernández et al., 2014), being narrowest in the vicinity of Garrucha Canyon head (GA). The shelf break in the Palomares margin is between 120 and 170 m depth, and the slope displays a complex morphology due to the presence of several submarine canyons (Aguilas (AGC), Alias-Almanzora and Gata), and prominent seamounts (Pérez-Hernández et al., 2014). In the Almeria margin, the continental shelf is 6 to 12 km wide (García et al., 2006), with the shelf edge at 100–120 m depth. The main geomorphological features therein are various submarine valleys which conform the Almeria Turbidite System (Estrada et al., 1997; García et al., 2006), which is the largest of its kind in the Alboran Sea (Vázquez et al., 2015).

From north to south and east to west the studied canyons are the N-S oriented single Escombreras Canyon on the Mazarron margin, the W-E Garrucha-Almanzora Canyon system (Fig. 2) that is the northern part of the Alias-Almanzora system on the Palomares margin, and the Almeria

Canyon on the Almeria margin (Fig. 1).

The Escombreras Canyon is more than 20 km long and mostly N-S oriented. It presents a maximum axial gradient of 15° . While the canyon head is convex in shape and it is cut by numerous gullies (Acosta et al., 2013), the lower canyon extends onto the uppermost continental rise where it forms a channel systems (Acosta et al., 2013).

The Alias-Almanzora Canyon system has a total length of 73 km (Pérez-Hernández et al., 2014) and consists of four shelf incised branches entering the Palomares margin. In its northernmost part, the Almanzora Canyon branch (ALM) converges at 1,100 m depth with the Garrucha Canyon branch (GA), resulting in the Garrucha-Almanzora system (following Puig et al., 2017 nomenclature). The Almanzora Canyon extends from 65 m depth off the Almanzora River (Puig et al., 2017) and presents a mean axial slope gradient of 8.6° and a total length of 8 km. The Garrucha Canyon branch splits in two canyon heads off the Almanzora River prodelta, together with two other main canyon heads further south, located between Antas and Aguas river mouths, opening as closer as 30 m from Garrucha harbor. The southern canyon heads are fed by several small tributary channels that could be tracked up to 7 m depth on the innermost shelf. The Garrucha Canyon branch displays a meandering pattern, with an average axial slope of 5° , for a total length of 15.7 km (Puig et al., 2017). At 1,811 m depth the Garrucha-Almanzora system merges with the southern Alias-Cabrera system, thus forming the Alias-Almanzora system (Pérez-Hernández et al., 2014).

The NE-SW oriented Almeria Canyon is more than 55 km long (García et al., 2006). Its axial gradient ranges between 1.2° and 1.4° , and it is fed by three tributary valley systems (TVS), from west to east, Dalias, Andarax and Gata (Fig. 2), which incise the shelf break and converge with the main canyon at 700–1,500, 300 and 650 m, respectively (García et al., 2006). The Dalias TVS covers an area of 300 km² with a length of 22 km, but only the Andarax TVS is connected to the Andarax River (García et al., 2006). The Almeria Canyon axis is NE-SW oriented down to 1,200 m depth where it becomes the Almeria Channel feeding a fan lobe system (Cronin et al., 1995; Estrada et al., 1997).

Thus, submarine canyons located in these margin segments are diverse in several aspects, such as size, orientation, with or without shelf incision, individual or with several tributaries and their relation with present day tectonics.

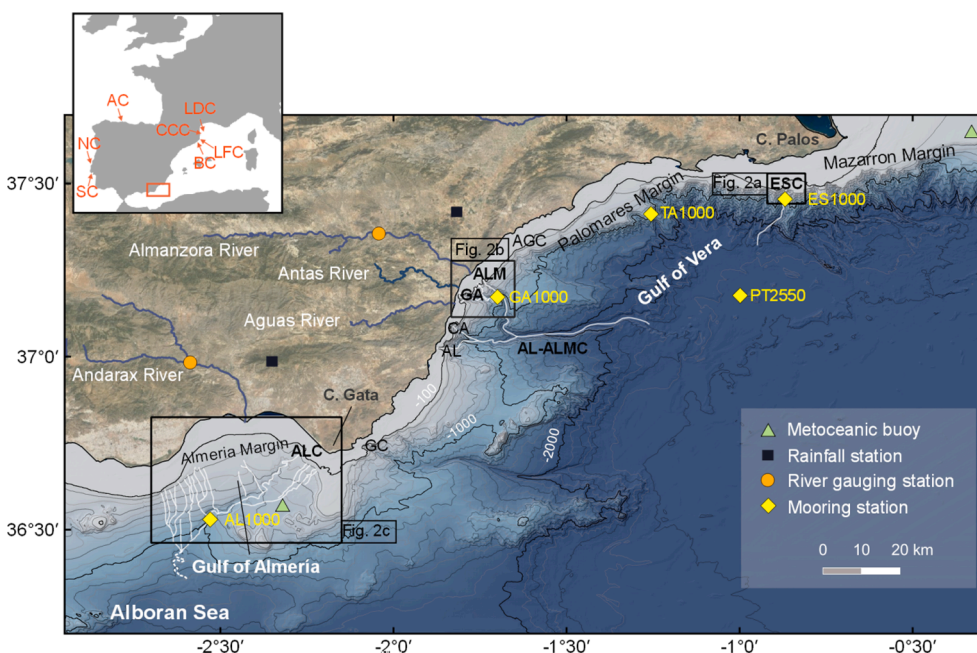


Fig. 1. Bathymetric map of the gulfs of Vera and Almeria with the main axis of Escombreras (ESC), Alias-Almanzora (AL-ALMC) and Almeria (ALC) canyon systems (white lines). The location of the Alias-Almanzora Canyon tributaries (AL: Alias; CA: Cabrera; GA: Garrucha; ALM: Almanzora) and the Aguilas Canyon (AGC) and the Gata Canyon (GC) are indicated. Yellow diamonds indicate the location of mooring stations. Cape of Palos and Cape of Gata metoceanic buoys (green triangles), rainfall stations (black squares) and river gauging stations (orange dots) are also shown. Black squares show the location of detailed submarine canyon maps in Fig. 2. Other submarine canyons referred to in this paper are shown in the inset (LDC: Lacaze-Duthiers Canyon; CCC: Cap de Creus Canyon; LFC: La Fonera Canyon; BC: Blanes Canyon; NC: Nazaré Canyon; SC: Sétubal Canyon; AC: Avilés Canyon).

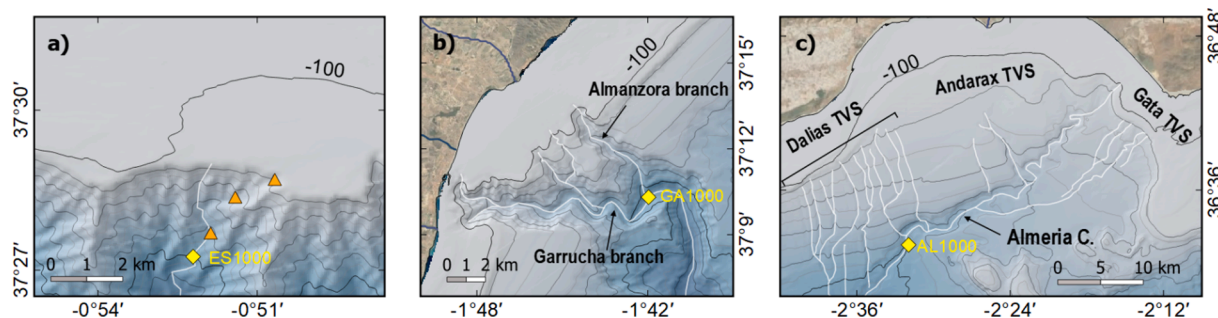


Fig. 2. Bathymetric maps of the heads of (a) Escombreras Canyon, (b) Garrucha-Almanzora Canyon system, and (c) Almeria Canyon and tributary valley systems (TVS). Yellow diamonds show the location of mooring stations and CTD deployments. Orange triangles illustrate a CTD transect across the outer Mazarron shelf and upper Escombreras Canyon. Yellow diamonds indicate the mooring sites.

3. Materials and methods

3.1. Experimental design

Three mooring lines were deployed along the axis of three submarine canyons at approximately 1,000 m depth: in Escombreras (ES1000), Garrucha-Almanzora (GA1000) and Almeria (AL1000) submarine canyons (Fig. 2). Two additional moorings were deployed as control stations, one in the open slope in the Palomares margin (TA1000) and one in the deep basin at 2,550 m depth (PT2550). The moorings were deployed from March 2015 to March 2016, with recovery-redeployment operations at month 6 for maintenance, changing batteries and sampling cups (Table 1). Each mooring was equipped with a Technicap PPS3/3 sequential sediment trap (0.125 m², cyliandroconical shape) with 12 trap cups with a sample resolution of 7–16 days. The mooring deployed in the deep basin was equipped with two sediment traps: one at mid-water depth (PT2550-S, with “S” standing for “shallower”) and the other near the bottom (PT2550-D, with “D” standing for “deeper”). The trap cups were filled with 5% (v/v) formaldehyde solution in 0.45 μm filtered sea water buffered with sodium tetraborate. Aquadopp Nortek current meters with sampling interval of 30 min were placed 2 m below the sediment trap to monitor current velocity, direction, pressure and water temperature. Some currentmeters were equipped with Seapoint turbidity meters, calibrated for Formazin Turbidity Units (FTU), which detect light scattered at 15°–150° (with a sensibility peak at 90°) of a confined volume of five centimetres of the sensor window. Pitch and roll parameters and velocity have been checked to assess that hydrodynamic conditions did not have a detrimental impact on trap verticality and discard a bias in the collection of particle fluxes (Gardner, 1985; Baker et al., 1988; Buesseler et al., 2007).

CTD (Conductivity-Temperature-Depth) profiles were carried out during 13th–23rd March 2015 and 29th August–1st September cruises around each mooring station. Additionally, a transect of 3 CTD casts comprising the outer area of the Mazarron margin and Escombreras Canyon was performed in March 2015 (Fig. 2a). The CTD was a SBE 911

Table 1

Metadata of mooring lines. Sediment traps were placed 25 mab (m above the bottom) except for PT2550-S level, which was at 546 mab (mid-water deep basin trap). Due to specific technical failures of the rotation system of sediment traps, the complete time series is not available for ES1000 and GA1000 mooring stations. Currentmeters were deployed below each sediment trap excepting in PT2550-S. Each currentmeter was equipped with turbidity meters excepting in AL1000. In PT2550, “S” stands for “shallower” and “D” stands for “deeper” (see further details in the main text).

Mooring station/ level	Latitude	Longitude	Mooring depth (m)	Minimum distance from mooring line to coastline (km)	Sampling period	Number of samples
ES1000	37°27.309'N	0°52.274'W	985	14	16/3/2015–28/8/2105	12
TA1000	37°24.613'N	1°15.394'W	1003	16	16/3/2015–31/3/2016	24
GA1000	37°10.294'N	1°41.968'W	1100	10.7	25/3/2015–15/10/2015	14
AL1000	36°31.709'N	2°32.003'W	1000	22	25/3/2015–31/3/2016	24
PT2550-S	37°10.635'N	0°59.993'W	2550	40	16/3/2015–31/3/2016	24
PT2550-D	37°10.635'N	0°59.993'W	2550	40	16/3/2015–31/3/2016	24

equipped with a WET Labs ECO-AFL/FL fluorimeter, a SBE 43 oxygen sensor and a WET Labs ECO-NTU turbidity meter sensor (in Nephelometric Turbidity Units). The turbidimeter measures turbidity from side-scattered light at 90° relative to the laser light.

3.2. Sample treatment and analytical procedures

Sediment trap samples were stored in the dark at 2–4 °C, and were processed in the laboratory following a modified protocol from Heussner et al. (1990), as described in Lopez-Fernandez et al. (2013b).

Total Mass Fluxes (TMF) were calculated for each period following next equation:

$$TMF (gm^{-2}d^{-1}) = \frac{\text{Sample dry weight}(g)}{\text{Collection area}(m^2) * \text{sampling interval}(d)} \quad (1)$$

Time weighted Fluxes (TWF) represents a weighted average corrected according sampling interval value:

$$TWF (gm^{-2}d^{-1}) = \frac{\sum M_i(g)}{\text{Collection area}(m^2) * \sum D_i(d)} \quad (2)$$

where: M_i is the mass of each sample and D_i is the collection interval days of each sample.

The contents of total Nitrogen (N), Organic Carbon (OC) and Total Carbon (TC) were determined using an Elemental Analyser EA Flash series 1112 in the Scientific and Technological Centres of the University of Barcelona. Before analysis, samples for OC determination were decarbonated with repeated additions of 10 μl of HCl (1 M) with 3 h 60 °C drying steps in between until no effervescence was observed. Percentages of organic matter (OM) and calcium carbonate (CaCO₃) were calculated following relations:

$$OM = OC \times 2 \quad (3)$$

and

$$\text{CaCO}_3 = (\text{TC} - \text{OC}) * 8.33 \quad (4)$$

where 8.33 is the molecular mass ratio (assuming that all inorganic carbon is in the form of calcium carbonate).

Biogenic Si content was obtained analysing Si and Al with an Inductive Coupled Plasma Optical Emission Spectroscopy (ICP-OES), with a two-step digestion for 2.5 h at 90 °C with a solution of Na₂CO₃ (0.5 M) following Fabres et al. (2002). Lixiviate Si/Al ratios were used as correction factor to obtain biogenic Si in sediments (Kamatani and Oku, 2000) and multiplied by factor of 2.4 to obtain opal percentage (Mortlock and Froelich, 1989). The opal fraction was determined in the PT2550-S samples, where pelagic sedimentation is expected to be more noticeable. In this case, the lithogenic fraction was calculated assuming that.

$$\% \text{lithogenics} = 100 - (\% \text{OM} + \% \text{CaCO}_3 + \% \text{opal}) \quad (5)$$

In the samples collected in the near-bottom traps, discrete analysis indicate a minor opal contribution to total mass. Then, the lithogenic fraction was calculated without considering this fraction.

Grain size analysis of particles were carried out with a Beckman Coulter LS 230 laser diffraction particle size analyser, which measures sizes between 0.04 and 2,000 µm. Prior to analysis, samples were twice oxidized with 50 ml of 10% H₂O₂, drying the samples between each oxidation. Each sample was then divided in two subsamples, one of which was de-carbonated with 50 ml 1 M HCl to obtain the grain size distribution of lithogenic particles. Once dry, both fractions were dispersed with 50 ml of 5% sodium polyphosphate solution and placed in a rotary agitating for at least 3 h to prevent particle's flocculation.

3.3. Metoceanic and human activity records

Metoceanic data (wind velocity and provenance, significant wave height and wave provenance) were obtained from *Agencia Estatal de Meteorología* and *Red de Boyas de Aguas Profundas* (REDEX, *Puertos del Estado*). In this study we used data from the Cabo de Palos buoy (Long. 0.33°W, Lat. 37.65°N), moored in the inner shelf of the northern margin of Gulf of Vera, and the Cabo de Gata buoy (Long. 2.32°W, Lat. 36.57°N) near Cape of Gata. In order to obtain accurate daily wave parameters close to the submarine canyons heads, 3 WANA points were used for this study. The WANA network delivers time series of wind and waves parameters from numerical modelling generated by *Puertos del Estado* in collaboration with *Agencia Estatal de Meteorología*.

Hourly Andarax and Almanzora river discharges were obtained from *Red SAIH Hidrosur*, operated by Junta de Andalucía. Gauging stations are not located near the river mouth. The above data was complemented with rainfall data from two meteorological stations located in the Almería province, from the same data source.

Monthly chlorophyll-a concentration (Chl-a) (mg m⁻³) and sea surface temperature (SST) (°C) data were obtained from Moderate Resolution Imaging Spectrometer (MODIS), in orbit on the Aqua platform, using 4 km resolution level 3 binned data. These data are processed and distributed by *NASA Goddard Earth Science (GES) Data and Information Services Centre (DISC)* and supported by the Ocean Biology Processing Group (OBPG).

Fishing activity has been monitored from Vessels Monitoring System (VMS) data provided by *Secretaría General de Pesca, Ministerio de Agricultura, Alimentación y Medio Ambiente* of the Spanish Government.

4. Results

4.1. Forcing conditions

Beyond major storms with high H_s (cf. section 2) the dry or wet character of every storm also is of relevance, as it defines the absence or presence of associated rainfall (Guillén et al., 2006). Indeed, eastern storms are charged with humidity and trigger precipitation by

orographic control when encountering the land, conversely to storms coming from mainland, i.e. from the north and west. Rainfall rates are often higher during late summer and autumn, when the evaporation of the relatively warm Mediterranean Sea provides a continuous supply of heat and water vapor, increasing the moisture content at low levels (Hermoso et al., 2021). However, as shown in Fig. 3, rainfall does not always translate into an increment of river discharge, since other factors such as infiltration and ground water reserves influence surface runoff and the fluvial response in dry climates such as the one in the study area (Liquete et al., 2005). During the studied period, three main stormy periods occurred (Fig. 3).

The first period developed in early spring 2015, mainly associated with north-eastern winds and characterized by unstable cold weather with various rainfall episodes. On 17-21th March 2015 the buoys registered a wet northern storm with H_s up to 4.8 m (T_s = 6.3 s) in Cape of Palos, exceeding 2 m for 77 h. In Cape of Gata the event had a maximum wave height of 4.2 m and less duration. After the storm, Andarax River registered a slight increase in discharge, with a maximum of 2.2 m³ s⁻¹. Two other wet storms occurred in April, the first between 6 and 9th, with a considerable duration of 88 h, was strongest in Cape of Gata with a maximum H_s of 4.5 m (T_s = 6.6 s), followed by a milder event on the 12th that was only recorded in Cape of Gata.

The second stormy period took place in autumn months and was characterized by a set of storms accompanied by abundant rainfall episodes, which impacted river discharge during September. On the first of November 2015 a north-eastern storm triggered H_s of 4.2 m at Cape of Gata and 3.9 m at Cape of Palos, lasting 37 h and 28 h, respectively. After the event both gauge stations registered a flood episode of up to 36.1 m³ s⁻¹ in Almanzora River and a less marked increment of 0.7 m³ s⁻¹ in the Andarax River. In late November another storm (H_s ≤ 4 m) of short duration (13 h) from the southwestern was recorded at the Cape of Gata buoy.

The last stormy period occurred during winter months early in 2016, driven by several strong wind episodes blowing from west and south, accompanied with rather weak rainfall, especially in the southern part of the study area. A set of events took place in early January, February and March. Near Cape of Palos occurrence and intensity were less, with maximum H_s of 4 m on 12th and 26th February. In Cape of Gata the strongest ones happened on the 7th, 9th and 19th February. In particular, the 9th February storm lasted for 149 h with maximum H_s of 4.8 m and T_s of 6.4 s. The rest of the events during February and March were milder, never surpassing a H_s of 3.7 m.

Concerning primary production, in early spring 2015 a bloom developed close to the coasts (Fig. 4), with maximum values up to 0.6 mg m⁻³ in March. Between May and October 2015, oligotrophic conditions prevailed in the study area, with relevant primary production outside the study area, in the south-western Alboran Sea associated to the WAG upwelling zone. An increment of chlorophyll-a at the sea surface occurred from November 2015 to March 2016, restricted to the Alboran Sea during autumn months and extending to the wide Gulf of Vera during winter months in early 2016. This bloom was particularly prominent during January near Cape of Gata and over Mazarrón margin, with Chl-a concentration up to 2.7 mg m⁻³, and low sea surface temperature (SST) near the coast.

4.2. Near bottom currents

Current velocities recorded in all stations did not exceed 20 cm s⁻¹, and only punctually reached more than 10 cm s⁻¹ (Fig. 5a-d). Current-meters deployed on the continental margin registered two periods with moderate increments of current speed, first during March-April 2015 and second during February-March 2016, as shown in stations with complete time series. In the deep basin station, the maximum current velocity was recorded at the end of April 2015, up to 19.5 cm s⁻¹, with current pulses coming from continental margin areas located to the north and west of the mooring site.

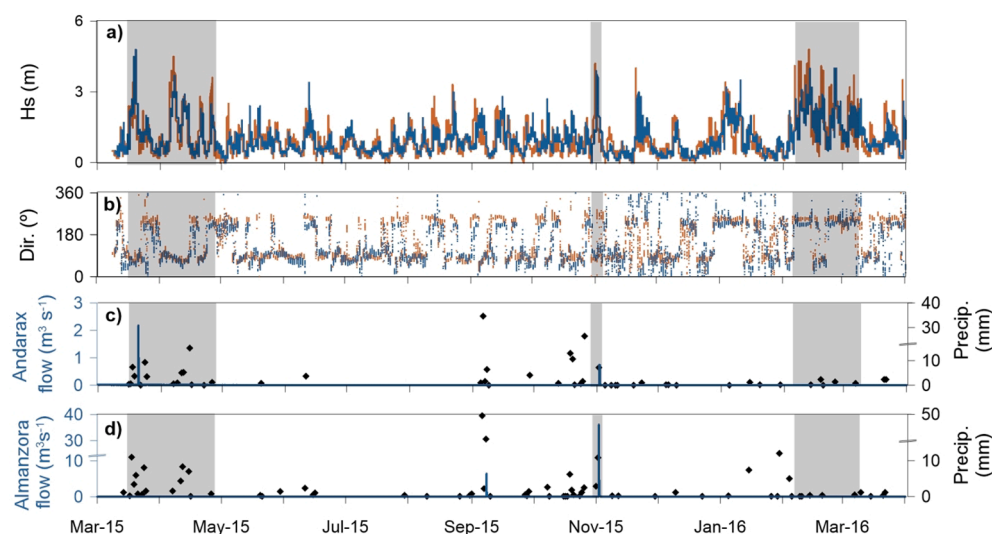


Fig. 3. Time series of external forcings during the year-round monitoring period from March 2015 to March 2016. (a) Significant wave height (H_s) at Cape of Palos buoy (orange curve) and Cape of Gata buoy (blue curve); the grey vertical stripes highlight the main storm events. (b) Wave provenance in Cape of Palos and Cape of Gata buoys. (c) Andarax River flow (Terque gauging station) and hourly accumulated precipitation (Rambla de Tabernas station). (d) Almazora River flow (Cantoria gauging station) and hourly accumulated precipitation (Sierra Almagro station).

Current velocity peaks did not coincide with turbidity peaks (Fig. 5a-c). The turbidity series generally present low values with subtle increases that did not surpass 3 FTUs, a tendency only disrupted in the Garrucha-Almazora Canyon. After late July, there was a progressive increase with a peak of 28 FTU at the end of August, followed by a quick decrease until reaching previous values in the last days of August 2015 (Fig. 5c). Biofouling is discarded to be the cause of the FTU increment observed in GA1000 because the subsequent flattening of turbidity values is not associated to a current speed increase that eventually could have swept away particles loosely adhered to the sensor.

4.3. Spatial and temporal variability of total mass fluxes

TMF's in the stations located in the continental margin were one order of magnitude larger than those in the deep basin. Basic statistics (Table 2) show a weighted average value (TWF) of $7.33 \text{ g m}^{-2} \text{ d}^{-1}$ in GA1000 whereas the one found in ES1000 is up to $4.80 \text{ g m}^{-2} \text{ d}^{-1}$. AL1000 presents a lower value than the two previous stations ($1.64 \text{ g m}^{-2} \text{ d}^{-1}$), similar to that obtained in TA1000 ($1.90 \text{ g m}^{-2} \text{ d}^{-1}$). Traps deployed at two levels in the deep basin (PT2550-S and PT2550-D) present TMFs lower than $1 \text{ g m}^{-2} \text{ d}^{-1}$ during all the monitoring period.

TMF values fluctuate considerably throughout the studied period (Fig. 6). The maximum values were recorded in March and April 2015. The maximum value was obtained in ES1000, up to $24.96 \text{ g m}^{-2} \text{ d}^{-1}$, followed by GA1000 ($18.15 \text{ g m}^{-2} \text{ d}^{-1}$), TA1000 ($8.37 \text{ g m}^{-2} \text{ d}^{-1}$) and AL1000 ($5.12 \text{ g m}^{-2} \text{ d}^{-1}$). Two behaviours are noted for the rest of the months. ES1000, AL1000 and TA1000 stations registered much lower fluxes during the rest of the monitoring period, with a minimal increment during autumn and winter months. In ES1000 station the lack of data prevents us from describing TMFs. Unlike those stations, fluxes recorded in GA1000 fluctuated during spring and summer months, until October. A different behaviour is observed in the deep basin station, with maximum values recorded in April 2015 in PT2550-S and September 2015 in PT2550-D.

4.4. Characteristics of settling particles

4.4.1. Main composition

At the canyon and open slope stations the lithogenic fraction is the main component (Table 2 and Fig. 6), with an averaged content of 72.4% in AL1000, and more similar percentages in the rest of the stations (60.5–65.0%). The averaged CaCO_3 content varies from 22.7% in PT2550-S and 36.5% in ES1000. OM percentages are lower in open slope and canyons stations (3.0–4.1%) while higher values have been found in

deep basin traps (5.7%). Analyses of some discrete samples from continental margin stations indicate that opal contents are negligible in those stations, with maximum values below 2.5%. In contrast, PT2550-S shows average opal values of $7.4 \pm 5.0\%$.

The molar OC/N ratio is represented in Fig. 6. Settling particles in GA1000 show values higher than 12 in almost the entire monitoring period, with a maximum of 20.1 in early April. In contrast, values in ES1000 and AL1000 samples are below 12. The OC/N ratio tends to diminish after March and April 2015, except in GA1000 station, which presents high values in August 2015 samples. TA1000 settling particles show the widest range (6.7–20.3), with more extreme values during the second deployment period. Concerning deep basin settling particles, PT2550-S shows lower values than PT2550-D, with an average of 9.0 against 9.8, respectively. In both sediment traps there was a tendency to increase OC/N ratios across the study period, with the exception of punctual PT2550-D samples.

4.4.2. Grain size of settling particles

The fine-medium silt fraction dominates de-carbonated samples at all traps and stations (Table 2). The finest grains are found in TA1000 and ES1000 settling particles, where the clay fraction averages 31.1% and 35.0%, respectively. GA1000 and AL1000 samples have more silt (74.0% and 81.2%, respectively) and sand fraction (2.3% and 3.1%, respectively). The averaged mean of the particles is coarser in AL1000 ($16.2 \mu\text{m}$), followed by GA1000 ($14.1 \mu\text{m}$), TA1000 ($12.9 \mu\text{m}$) and then ES1000 ($9.3 \mu\text{m}$).

The average grain size distribution during stormy periods (Fig. 3) does not show significant variations (Fig. 7). Concerning spring 2015 storms, the main mode was fairly coarse during March 2015 at ES1000 and AL1000 stations, with means of $11.3 \mu\text{m}$ and $21.1 \mu\text{m}$. In posterior storm events only settling particles collected in TA1000 in early February 2016 show a higher mean ($24.5 \mu\text{m}$).

4.5. Water column parameters

Suspended particulate matter distribution has been obtained from turbidity meters attached to the CTD in March 2015 and late August 2015 (Fig. 8). In March 2015, we observe differences between the CTD casts performed the 13–14th March (TA1000 and ES1000), which show fairly constant turbidity values along the water column around 0.2 NTU, and casts conducted the 20th–23rd March at ES1000 and GA1000 stations, showing an increase of turbidity within continental shelf depths. During that period, the CTD transect along the Escombreras Canyon (Fig. 9c) reveals higher turbidity values (up to 3.74 NTU) near bottom

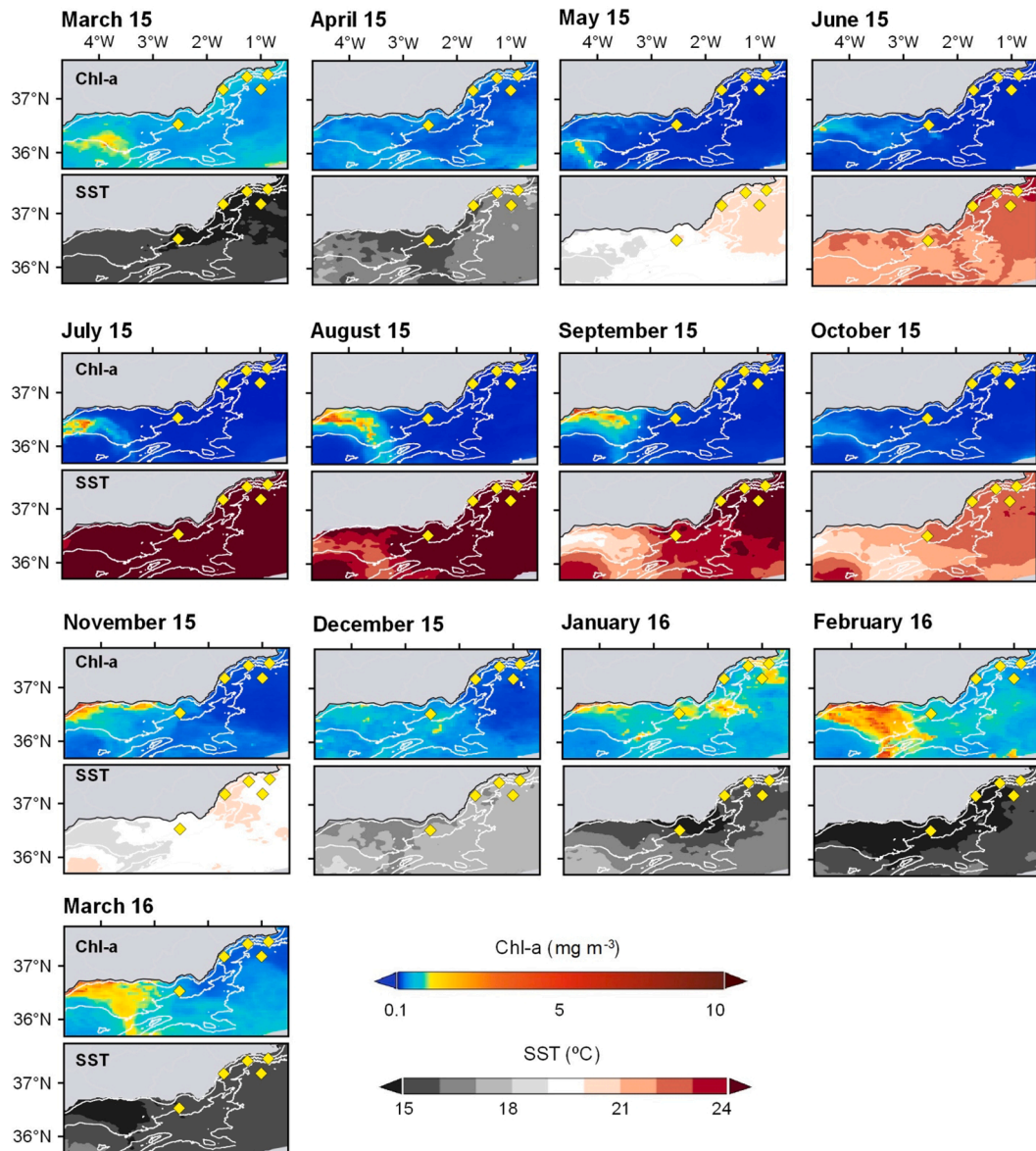


Fig. 4. Monthly averaged superficial chlorophyll-a concentration maps (mg m^{-3}) and SST ($^{\circ}\text{C}$) from March 2015 to March 2016. The yellow diamonds represent the mooring lines.

on the outer continental shelf, with turbidity diminished seawards, reaching 1.14 NTU in the last CTD deployed near the ES1000 station. CTD casts near GA1000 station peak at 0.56 NTU, to gradually decrease below the shelf break until reaching values similar to those of the deep basin. Moreover, turbidity values near GA1000 began increasing again below 400 m depth, extending hundreds of meters down to the bottom, while reaching values up to 0.32 NTU. The CTD cast performed near AL1000 has shown quite constant turbidity values along the water column.

The hydrological parameters of the upper 1,000 m of the water column also vary notably between the 13–14th and the 20th–23rd March 2015 CTD deployments (Fig. 8), as shown by stations ES1000 and TA1000 on one side, and stations GA1000 and ES1000 on the other side. The exception are profiles from AL1000 of the 23rd of March, which are more similar to the ones from ES1000 and TA1000 about 10 days earlier. It should be noted here that AL1000 is quite far from the broad area where the rest of stations are located (Fig. 1). Profiles in Fig. 8 allow identifying a number of water masses, including a surface layer, a sub-surface layer and the Levantine Intermediate Water (LIW). Most interesting are the 20th and 22nd of March GA1000 and ES1000 profiles,

showing surface water mass down to about 200 m with relatively high potential temperature ($13.65\text{--}13.80^{\circ}\text{C}$) and fairly low salinity ($38\text{--}38.1$ psu), coinciding with a layer-thick fluorescence and, especially, turbidity increase (Fig. 8). Below is a sub-surface layer down to 300 m depth, made of almost mixed, colder and oxygen-rich water (minimum temperature of 13.17°C), less saline ($38.15\text{--}38.25$ psu). Finally, the deeper LIW is indicated by a relative maximum in temperature and a relative minimum of dissolved oxygen. Fig. 9 a, b, d shows the variation of θ/S and DO seaward over Escombreras Canyon.

During the late August/early September 2015 cruise, the CTD casts at TA1000 and AL1000 did not show significant differences compared to deep basin values. However, the CTD cast at GA1000 once again presented a turbid layer under 400 m, with a maximum value of 0.37 NTU between 600 and 750 m and an increase of 0.39 NTU near bottom.

Fluorescence profiles indicate phytoplankton blooms. In mid-March 2015 maximum chlorophyll values were located near the surface with higher values, up to 1.38 mg m^{-3} , over Escombreras Canyon. At the end of March 2015, the fluorescence signal was weaker and distributed along the water column until 250 m depth (Fig. 8d). During late summer deployments the fluorescence peak was between 80 and 90 m depth,

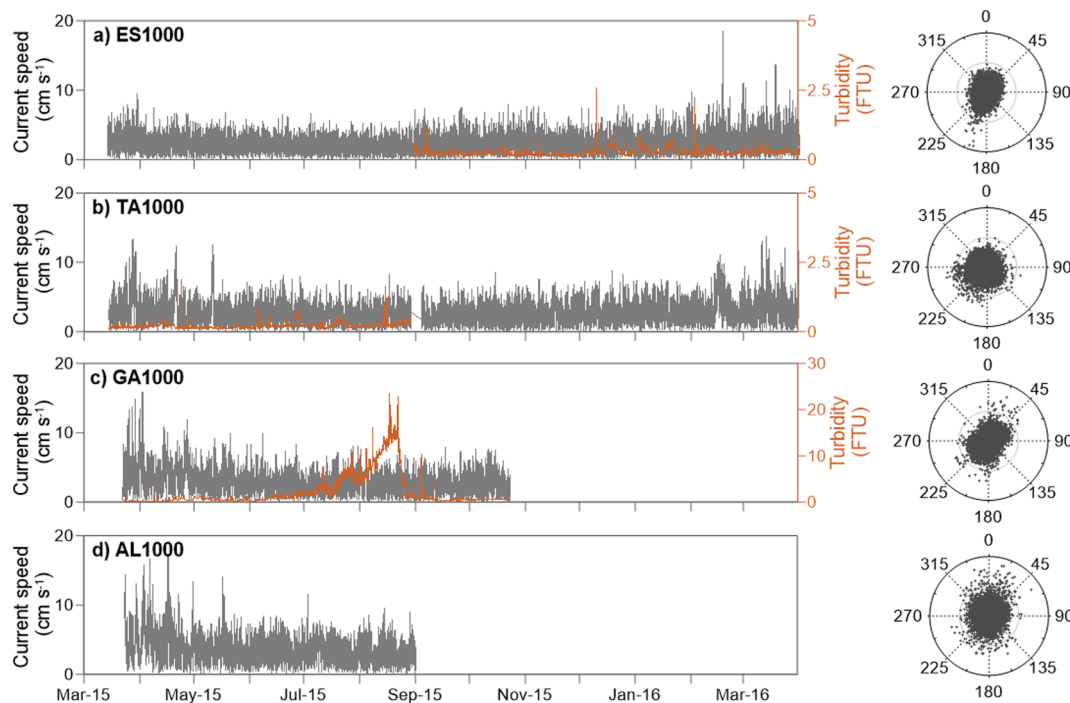


Fig. 5. Current speed (grey line) and turbidity (orange line) recorded at 20 mab in (a) ES1000, (b) TA1000, (c) GA1000 and (d) AL1000 stations. Polar plots show the direction of currents with the X axis ranging from 0 to 20 cm s^{-1} . FTU: Formazin Turbidity Units.

Table 2

Averaged total weighted flux (TWF), averaged total weighted components (TWC), and grain size of the de-carbonated fraction of samples from each sediment trap. Standard deviation is also shown. Note that the series only cover from March to September 2015 in the GA1000 station and from March to August 2015 in the ES1000 station.

Mooring station/sediment trap	TWF $\text{g m}^{-2}\text{d}^{-1}$	Components (TWC)				Grain size (de-carbonated)		
		Litho %	CaCO ₃ %	OM %	Opal %	Clay %	Silt %	Sand %
ES1000	4.80 ± 6.55	60.5 ± 2.7	36.5 ± 3.1	3.0 ± 0.8	–	35.0 ± 2.7	65.0 ± 2.7	null
TA1000	1.90 ± 1.61	60.6 ± 7.3	36.3 ± 8.1	3.1 ± 0.9	–	31.1 ± 6.9	66.9 ± 5.7	2.0 ± 3.7
GA1000	7.33 ± 5.31	62.4 ± 3.2	34.2 ± 3.8	3.4 ± 0.9	–	23.7 ± 4.0	74.0 ± 3.4	2.3 ± 1.2
AL1000	1.64 ± 1.32	72.4 ± 2.1	23.5 ± 2.1	4.1 ± 1.1	–	15.8 ± 5.7	81.2 ± 4.7	3.1 ± 1.7
PT2550-S	0.07 ± 0.12	64.2 ± 10.1	22.7 ± 11.4	5.7 ± 2.9	7.4 ± 5.0	–	–	–
PT2550-D	0.06 ± 0.05	65.0 ± 9.1	29.3 ± 8.8	5.7 ± 2.1	–	–	–	–

with peak values reaching 1.59 mg m^{-3} near GA1000 station, 1.01 mg m^{-3} near TA1000 and 0.75 mg m^{-3} near AL1000.

5. Discussion

5.1. Sources of particulate matter

Temporal variability of particle fluxes in continental margins, and in Mediterranean margins in particular, follows deposition and remobilization cycles involving the transfer of matter and energy from the shelf to the slope and deep basin, as pointed out by several authors (Heussner et al., 2006; Ulses et al., 2008; Palanques et al., 2012; Puig et al., 2014). This leaves an imprint on grain size and the biogeochemical characteristics of the settling particles. Indeed, the grain size of settling particles has been related to lateral transport and sediment sorting (Ferré et al., 2005; Guillén et al., 2006; Sanchez-Vidal et al., 2012; Pedrosa-Pàmies et al., 2013). Also, some biogeochemical parameters are often used as proxies to identify the sources of particle-forming materials. The OC/N ratio in particulate matter is one of these proxies, which allows distinguish between marine and terrestrial OM. Vascular plant-derived OM is typically depleted in nitrogen (molar OC/N ratio > 16), whereas phytoplankton sourced OM shows higher nitrogen contents (molar OC/N ratio < 7) (Goñi and Hedges, 1995). Furthermore, the tendency of

vascular plant detritus to preferentially gain N during soil microbial decay may decrease the OC/N ratio from the originating plants down to 8 (Hedges et al., 1997; Sanchez-Vidal et al., 2013). Therefore, grain size and OC/N ratios allow achieving a rather incisive view of the processes affecting particle fluxes in settings such as the one of the study area.

The grain size distribution of de-carbonated settling particles shows that fine particles dominate in canyons (Table 2), in accordance to the calm hydrodynamic conditions during the investigated year-round period. Also, low grain size standard deviation is indicative of fairly stable hydrodynamic conditions at least at the depths where sediment traps were deployed. The lithogenic fraction dominates in all stations, pointing to a high relative contribution of terrestrial inputs along the investigated continental margin. Nonetheless, the terrestrial contribution probably is higher if we take into account that carbonate rocks are abundant in the watersheds feeding the study area, especially to the north. Thus, part of the calculated CaCO₃ fraction likely derives from detrital carbonates. As it can be seen in Table 2, the mean CaCO₃ values in submarine canyons (except Almeria Canyon) and open slope stations are about 11–14% higher than the one in the deep basin mid-water trap, where the highest biogenic contribution could be expected. Fluvial systems are a major source of terrigenous particles for submarine canyons which heads are at short distance from river mouths. These river-sourced particles easily reach mid-canyon segments. Particles settling

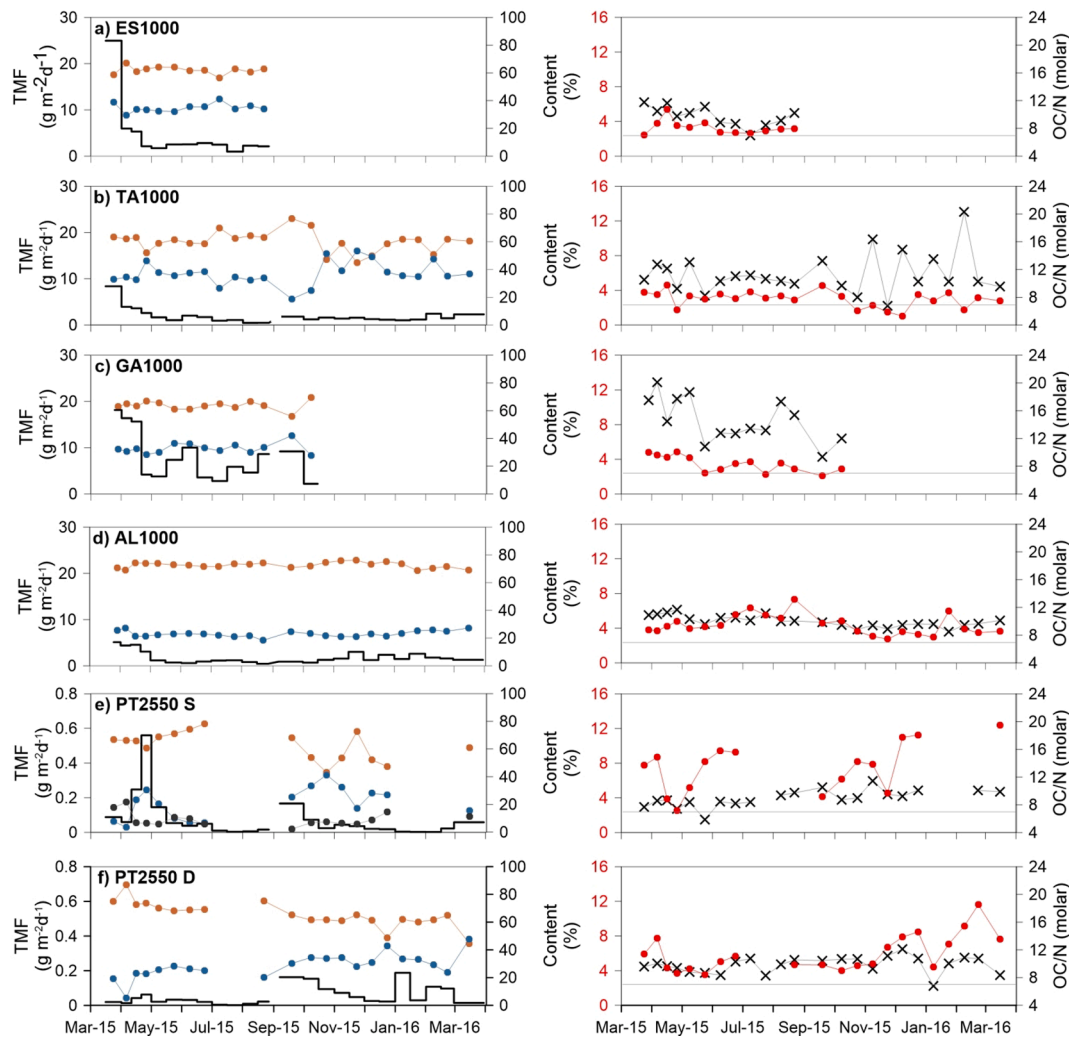


Fig. 6. Total Mass Fluxes (TMF) in the various traps deployed in mooring stations and percentages of lithogenics (brown line), CaCO₃ (blue line), opal (black line) and OM fractions (red line) in station (a) ES1000, (b) TA1000, (c) GA1000, (d) AL1000, (e) PT2550-S and (f) PT2550-D. Black crosses represent OC/N ratios. The grey line separates the OC/N ratios with values higher than 7 from the lower ones. OC/N < 7 is considered as indicative of OM from phytoplankton.

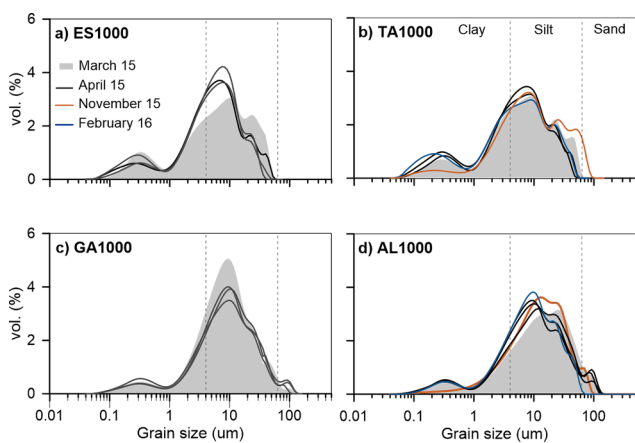


Fig. 7. Grain size distribution of the lithogenic components during stormy periods in Escombreras, Garrucha, Almeria and open slope sediment traps. The March 2015 sample is represented as shadow grey, April 2015 samples as black lines, early November 2015 as orange lines and early February 2016 as blue lines. The grey vertical dotted lines divide the clay (<4 µm) (fine-medium silt fraction between 4 and 40 µm) and sand fractions (63 µm–2 mm).

in the Garrucha-Almanzora Canyon show a clear terrestrial imprint, with OC/N ratios between 9.3 and 20.1 (Fig. 6). Lower OC/N ratios are found in settling particles in Almeria (8.5–11.7) and Escombreras (6.9–11.8) canyons. While the lowest values indicate punctual periods of non-degraded marine OC, most ratios found are compatible both with soil degraded OM and mixtures of OM from different origins. Settling particles collected in the open slope show larger heterogeneity of OC/N ratios (6.7 to 20.3). The higher OC/N ratios recorded during autumn and winter months suggest that materials entering the inner shelf through nearby *ramblas* with sporadic discharge events are able to reach the open slope.

The imprint of primary production on settling particles is not always obvious due to the dilution of pelagic marine materials within larger amounts of lithogenic particles carried by advective fluxes from the inner continental margin. Temporal variability of primary production results from shifts in hydrographic conditions throughout the year. Different regimes can be established in the three environments under consideration (i.e. submarine canyons, open slope and deep basin). The seasonal behaviour of settling particles is better recorded in open slope and deep basin samples, with periods where fluxes are dominated by fresh marine OM and biogenic components, which contrasts with prevailing homogeneity in canyon particle samples. Moreover, differences are also evident between near-bottom and mid-water traps in the deep basin (PT2550). Lower OC/N ratios found at mid-water depths

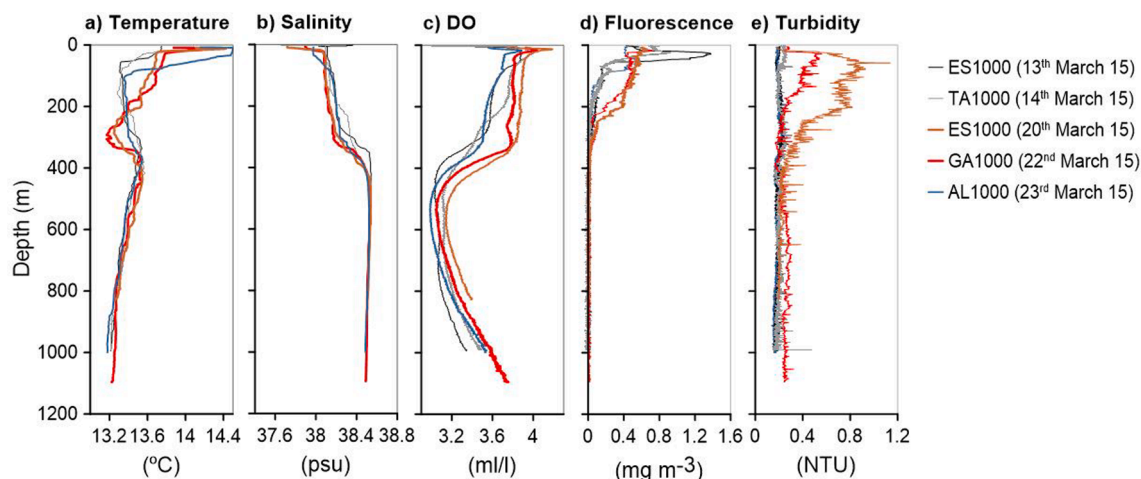


Fig. 8. Hydrological parameters (potential temperature, salinity, dissolved oxygen (DO), fluorescence and turbidity) from CTD transects during mid-March (pre-storm event; grey tones) and late March 2015 (post-storm event; red, purple and blue colours) at ES1000, TA1000, GA1000 and AL1000 stations. Note that AL1000 station is quite far from the rest of stations (Fig. 1).

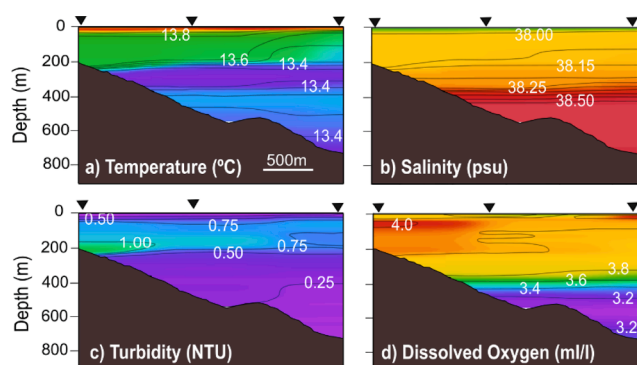


Fig. 9. Water column properties above the Escombreras Canyon transect after the March 2015 storm: a) Potential temperature (degrees). b) salinity (PSU). c) turbidity (NTU). d) dissolved oxygen (ml/l). The location of CTD casts is shown by the inverted black triangles.

compared to those obtained in the near bottom suggest a greater prevalence of pelagic settling at mid-water depth than at near bottom, and the ability of the terrestrial signal to be transferred to the deepest station under scrutiny, at depths larger than 2,000 m. Bottom transport of particulate matter to the deep basin in the western Gulf of Vera has been previously attributed to benthic nepheloid layers detaching from the nearby continental margin (Masqué et al., 2003; Sanchez-Vidal et al., 2005).

In March 2015, there was a reinforced primary production along the coastal area, as shown by satellite Chl-a maps (Fig. 4). In addition, sub-surface fluorescence in the deep basin showed values between 30 and 80 m deep that were higher than at surface. This is likely connected to the increase of CaCO_3 , OM and opal fluxes between late March and May 2015 in the deep basin mid-water station (546 mab) (Fig. 6). There is also a variation in the percentages of biogenic components throughout the sampling period, which could be attributed to planktonic community successions. Higher opal and OM percentages are recorded from the end of March to early April, which likely result from diatom-rich phytoplankton blooms (Fabres et al., 2002; Hernández-Almeida et al., 2011). Then OM and opal contributions diminish during the flux peak ($559.6 \text{ mg m}^{-2} \text{ d}^{-1}$) in late April, while the abundance of calcareous particles grows up. High phytoplankton productivity is likely to support the posterior development of zooplankton communities (Hernández-Almeida et al., 2011). This hypothesis fits with the visual inspection of the samples, which allow observing an increment of planktonic

foraminifera in that time. Such biogenic imprint is not detected in the deep basin near-bottom trap, suggesting some degree of uncoupling between middle and lower depths.

Between April and October 2015, superficial primary production was restricted to the WAG upwelling, whereas oligotrophy prevailed in the rest of the area (Fig. 4). In late summer, fluorescence profiles suggest the presence of a deep chlorophyll maximum (DCM) under the seasonal thermocline, a feature that has been widely observed in other parts of the Mediterranean Sea (Estrada et al., 1993). This is not shown satellite data, as these only illustrate surface pigment contents. Those conditions probably favoured the development of oligotrophic species that contributed to the increment of CaCO_3 contents and to higher N values during September in particles settling in the Garrucha-Almanzora Canyon (Fig. 6).

In November and December 2015 a widespread phytoplankton bloom occurred in the Gulf of Almeria (Fig. 4). Enhanced primary production during this period has been attributed to de-stratification and increased wind speed triggering fertilization events (García-Gorriz and Carr, 2001). Settling particles in Almeria Canyon do not show a biogenic imprint as it could be expected, even though there is a slight decrease of OC/N ratios with respect to previous samples. Concerning the open slope trap in station TA1000, there is a remarkable increment of CaCO_3 content (up to 51 and 53% of the total flux during late October and late November 2015, respectively) (Fig. 6). An increase of biogenic particles collected in sediment traps could be linked to direct pelagic input from surface blooms or to earlier blooms leading to deposition on the shelf followed by lateral transport (Martín et al., 2006; Bonnin et al., 2008). Nevertheless, it could be assumed that the contribution of pelagic fluxes is significant given the low OC/N ratios measured and the absence of energetic hydrodynamic conditions that could potentially increment advective near-bottom fluxes.

During January and February 2016, the prevalence of westerly winds induces favourable upwelling conditions along the coast (Sarhan et al., 2000; Baldacci et al., 2001). Nutrient-rich cold water tongues promoted pronounced local blooms in January, with superficial blooms concentrating west of Cape of Gata in February 2016 (Fig. 4). The arrival of pelagic material this time is detected in settling particles in the Almeria Canyon in late January, characterized by an increment (5.9%) of OM abundance and the lowest measured OC/N ratio (8.5) (Fig. 6). In the Gulf of Vera deep basin station, only the near-bottom trap recorded an increase in particle fluxes in early January ($188.1 \text{ mg m}^{-2} \text{ d}^{-1}$) with a low OC/N ratio (6.8). Despite this, the biogenic imprint on the composition of the particles is not evident. Satellite images indicate that the moored trap is located on the western edge of a highly productive area at

the sea surface, thus evidencing that collected particles had been transported by pelagic sedimentation involving both vertical and horizontal motion.

5.2. The role of oceanographic processes in sedimentary particle transfer

High waves and increased shelf current velocities are the prevalent hydrodynamic responses to strong winds, subsequently increasing bottom shear stress and triggering resuspension and transport of particles across and off-shelf (Guillén et al., 2006; Ulses et al., 2008; Palanques et al., 2008b; Sanchez-Vidal et al., 2012). Shelf-indented submarine canyons have the ability to intercept shelf sediment transport (Canals et al., 2013). Further, storm characteristics, river inputs and preceding oceanographic conditions determine sediment supply from the shelf to submarine canyons (Fabres et al., 2008; Palanques et al., 2008b; Puig et al., 2014; Rumín-Caparrós et al., 2016). In the study area, storm events were recorded during early spring and autumn 2015 and in winter 2016, as detailed below.

The first storm lashed out from March 17th to 21th during 77 h. Intense north-eastern winds strengthened the advection of water over the Gulf of Vera shelf following the general circulation in the area. 70 h from its start and 17 h after the maximum wave peak, CTD casts were performed around the Escombreras Canyon head, where water column turbidity showed increased values at intermediate depths (Fig. 9). This confirms the resuspension of particles due to wave action and their advection from the shelf break. A near-bottom increase of turbidity off the shelf-break was not noticed beyond 1,500 m (Fig. 9), indicating that near-bottom downcanyon sediment transport was constrained to the Escombreras Canyon head. The seaward transport of turbid shelf waters was further restricted to the surface layer, over the above-mentioned sub-surface layer of colder water (cf. section 4.5) that appears in all CTD profiles along the Escombreras Canyon axis (Fig. 9) and in the punctual CTD performed in Garrucha-Almanzora Canyon system after the storm (Fig. 8). This sub-surface layer could be tentatively related to Winter Intermediate Water (WiW) produced in the western Mediterranean during winter (Millot, 1999 and references therein) or to storm-induced downwelling, or both. Even though a clear WiW hydrological signature is not apparent in θ/S diagrams (Vargas-Yañez et al., 2017), a WiW warmer than 13 °C was detected south of the Balearic Islands during winter 2015 by Juza et al., (2019). Subsequently, the sub-surface layer in our study area can be interpreted as a WiW intrusion into the Gulf of Vera. It is also worth considering the role that the north-east storm may have played in the arrival of the WiW to our study area, taking into account the change in hydrological structure observed between mid-March (CTDs conducted 2–3 days before the storm) and late-March 2015 (CTDs conducted during and 1 day after the storm) (Fig. 8a, b and c). Therefore, our data indicates that the presence of the WiW had a noticeable impact on particle transport into the Escombreras and neighbouring canyons. Such a situation is somehow comparable to the one in canyons of the northern Catalan margin during autumn months, when the seasonal stratification of the water column hinders vertical displacements and restricts the storm-induced downwelling motion to canyon heads (Palanques et al., 2006a, 2008b; Bonnin et al., 2008; Ulses et al., 2008). However, the spatial resolution of the across-canyon CTD casts in our study is not adequate to study in detail the interplay between the WiW and downwelling at the upper canyon course.

Accordingly, in the Palomares margin, intense and persistent north-eastern winds may promote coastal downwelling, thus forcing turbid shelf waters to downwell into the heads of Garrucha-Almanzora Canyon system and other canyons nearby. Actually, the role of bottom advective currents in particle transport in the Garrucha-Almanzora Canyon system could be highly relevant, as Puig et al. (2017) found seabed landforms consistent with storm-induced sediment-laden density currents in the canyon heads. However, as noted previously, the presence of pycnoclines may restrict near-bottom suspended transport to the uppermost canyon. Increased downward particle fluxes after a storm may occur

when turbid layers pushing offshore isopycnal surfaces loose part of their suspended sediment load (Durrieu de Madron et al., 1990; Langone et al., 2016). This is fully consistent with the lack of enhanced bottom currents at ES1000 station and the low turbidity and bottom current velocities recorded at GA1000 (Fig. 5).

The views above are further supported by total mass flux measurements as related to the March 2015 storm (Fig. 6). Fluxes up to 24.96 g m⁻² d⁻¹ and 8.37 g m⁻² d⁻¹ were measured in the stations in Escombreras Canyon and the open slope (Fig. 6). Sediment traps moored in Garrucha and Almeria canyons opened with 2–3 days of delay with respect to the onset of the storm, recording fluxes up to 18.15 g m⁻² d⁻¹ and 5.12 g m⁻² d⁻¹, respectively (Fig. 6). The last values indicate that the transport event lasted several days while representing minima for particulate matter export. Again, it should be kept in mind that the setting of Almeria Canyon differs from the one of the rest of the investigated canyons.

Storms on the 6th and 12th of April 2015 triggered less particulate matter transport than the previous event according to sediment trap data (Fig. 6), likely due to the depletion of unconsolidated, easily resuspendable shelf sediments after the first event, as it would correspond to a sediment-starved marginal setting. Settling particles have higher OC/N ratios in all stations, except in Escombreras Canyon. This could relate to the replenishment of fresh sediments near river mouths during the flooding episode following the storm and subsequent sediment transport, as also observed in the inner shelf off Têt River in the Gulf of Lions (Guillén et al., 2006).

The spring 2015 storms increased the export of particles towards the deep basin all along the continental margin in the study area. However, there are noticeable differences from one margin segment to the other. TMFs recorded in Garrucha-Almanzora Canyon system were at least 1.5 times greater than in Escombreras Canyon, and 3 times greater than in Almeria Canyon, which is close to TA1000. The high values recorded in GA1000 station are linked to canyon heads' configuration, which are strongly indented in to the continental shelf, thus making this canyon system highly sensitive to shelf processes while favouring its interception and funneling capacity of shelf-derived particles. It should be also noted that whereas sediment traps in Garrucha-Almanzora and Escombreras canyons are at similar distance from the coastline (10.7–14.0 km), Almeria Canyon is at twice that distance. Moreover, wave data derived from the WANA model (<https://www.puertos.es>) for 2015–2016 near each canyon head document the generation of large waves under prevailing strong northeast winds around Escombreras and Garrucha canyons. Contrastingly, in the Gulf of Almeria only south-western storms are able to generate large waves. Coastal configuration there, with Cape of Gata promontory to the east likely acting as a shelter against north-eastern storms, leads to the reduction of wave heights, thus lessening the resuspension of bottom sediments that could potentially reach Almeria mid canyon stretch.

During subsequent stormy periods in autumn 2015 and winter 2016, only AL1000 and TA1000 sediment traps remained operational. The 1st and 21th of November 2015 storms were preceded by rainfall episodes. During the first event, H_s increased to 4.2 m and, following the event, Andarax River moderately incremented its discharge to the sea. A rather unusual situation took place during winter months in early 2016, with very low monthly average precipitation with respect to reference values within the same period (AEMET, 2016). The most remarkable storm in those months occurred in February 2016, when southwestern winds blowed during six days triggering a maximum H_s of 4.8 m near Cape of Gata (Fig. 3). The impact of the storms on particulate matter fluxes is not visible in either of the two sediment traps, AL1000 and TA1000 (Fig. 6). The short duration of the November 2015 events, always <37 h, largely explains the low sediment transfer from the shelf to these mooring stations. Other factors possibly played also a role in the low TMFs during February 2016 storms. The absence of rains during winter months prevented the arrival of new terrestrial material from the river systems to the inner shelf. This factor likely controlled, at least partly, particle fluxes in both stations and especially in the Gulf of Almeria, taking into

account the low discharge of Andarax River following autumn storms. Unlike the samples collected during autumn and winter in AL1000, those collected in TA1000 have high OC/N ratios, reaching up to 20.3 in early February (Fig. 6). Such high ratios support the arrival of terrestrial material deposited onto the inner shelf during previous floods to the mooring site.

5.3. The role of anthropogenic activities in sedimentary particle transfer

Studies developed in La Fonera Canyon, in the NW Mediterranean Sea, have shown that the impact of bottom trawling practiced in and around upper submarine canyon reaches is not restricted to those sections, but also affects deeper canyon sections and out of canyon continental rise areas (Palanques et al., 2006b; Puig et al., 2012; Payo-Payo et al., 2017). Detailed monitoring studies have reported sudden sediment gravity flows during summer months triggered by bottom trawling in that area (Palanques et al., 2006b; Puig et al., 2012). Similar situations have been described and / or inferred in and around other submarine canyons both in the Western Mediterranean Sea and beyond, such as Blanes Canyon (Lopez-Fernandez et al., 2013b) in the Catalan margin, Guadiaro Canyon (Palanques et al., 2005) in the Alboran Sea or the Avilés Canyon in Cantabrian margin (Rumín-Caparrós et al., 2016). The Garrucha-Almanzora Canyon system flanks are located at the edge of Verin and Canto Pote fishing grounds, where intensive bottom trawling takes place in the 500–800 m depth range (García-Rodríguez, 2005). Fishing interest for this canyon system relates to quasi-permanent subsurface upwelling conditions (Muñoz et al., 2018) together with its character of terrestrial OC depocenter, which result in fish aggregation and likely enhancement of local biodiversity.

Trawling-induced sediment resuspension probably is the mechanism that feeds the nepheloid layer below 400 m down to the bottom, as observed in late March and late August CTD casts. VMS data show that the majority of fishing vessels operate at 500–650 m of water depth along the canyon rims and adjacent slope, although during June and July they reach deeper regions around 800 m (Fig. 10). The number of vessel data points within a radius of 4 km around the Garrucha-Almanzora Canyon system mooring station increases during July and August (Fig. 10a). As a result, CTD turbidity values also augment at depths (600–750 m) slightly deeper than the peak of vessels in operation within the same period (Fig. 10b-c) and near the canyon floor. Near-bottom currentmeter measurements show a prominent bottom turbidity increment during summer months followed by a sharp decrease in late August (Fig. 5c). The reason for such a drastical diminution of turbidity is not obvious, since hydrodynamic conditions did not appear to change and there was no reduction in fishing activity. It is, however, plausible that the arrival of primary production particles from DCM contributed to the scavenging of suspended particles, which eventually resulted in the minimum OC/N ratio found in settling particles of September 2015 (Fig. 6). Unfortunately, the temporal resolution of sediment trap sampling prevents us from assessing in greater detail the interrelations of turbidity with other parameters.

It could be assumed that particles remobilized by bottom trawling come from different places, including the adjacent eastern and western open slope and the canyon flanks. Along slope currents passing over Garrucha Canyon would promote the arrival of particles from the eastern open slope into the canyon, as suggested by the persistent westerly currents recorded by the currentmeter in GA1000. The increase in fishing activity along the upper canyon walls during August 2015 explains the high OC/N ratios found in settling particles during that month (Fig. 6), which exceeds the rest of summer samples, and evidences that the material from upper regions is flushed downcanyon.

5.4. Particle flux comparison with other submarine canyons

The fluxes obtained in Escombreras, Garrucha-Almanzora and Almeria submarine canyons are clearly lower than those observed in

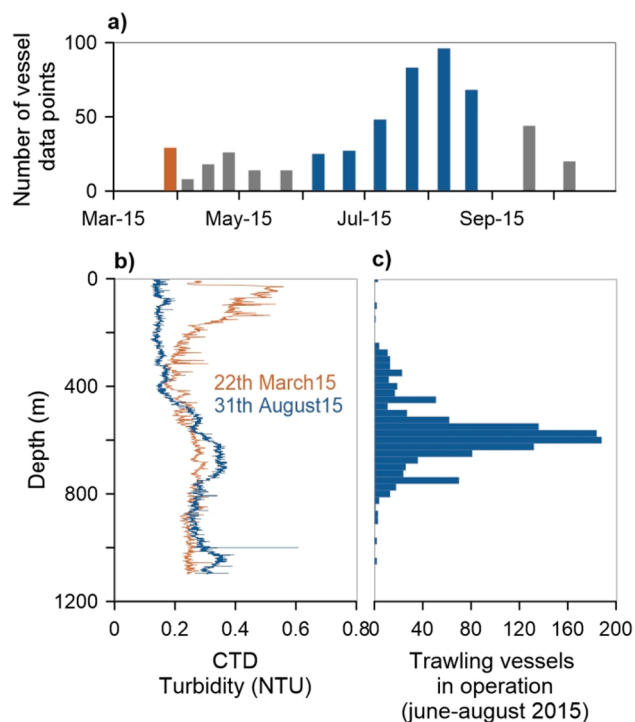


Fig. 10. (a) Number of VSM data points from fishing vessels within a radius of 4 km around GA1000 sailing at <5 knots (i.e. while trawling). (b) CTD turbidity profiles performed in March 2015 (orange) and August 2015 (blue). (c) Operating depth of trawling vessels between June and August within a radius of 4 km from the mooring line.

other canyons in the Western Mediterranean Sea, and also are in the lowest range of those found in canyons around the entire Iberian Peninsula (i.e. including three submarine canyons in the Atlantic Ocean). This is well illustrated when plotting weighted fluxes calculated in this study against those observed in other canyons (Fig. 11). It has to be noted that data from the Atlantic canyons reflect results from canyon reaches that are deeper than those from the Mediterranean Sea, so that it would be reasonable assuming higher fluxes in shallower canyon regions, as pointed by Heussner et al. (2006) for a set of submarine canyons in the Gulf of Lions.

Most submarine canyons in the North Catalan margin have their heads deeply incised in the continental shelf, as marked by small short distances to the shoreline in Fig. 11, except for Lacaze-Duthiers Canyon. This enables those canyons to trap large volumes of river-delivered sedimentary particles transported by littoral currents. Such trapping effect could be reinforced by specific external forcings and local conditions encompassing metoceanography, physiography, a variety of sedimentary processes and also anthropogenic forcing, as described above (Puig et al., 2014). In the Atlantic Iberian margin, also Nazaré Canyon and to a lesser extent, Setubal Canyon, are deeply incised into the continental shelf with their head at or at short distance from the shoreline.

The low particle fluxes recorded in the studied submarine canyons are highly influenced, first, by the scarcity of river inputs onto the shelf, which is ultimately related to the region's arid climate and weak river discharge. Annual precipitation in the watersheds opening to the investigated continental margin are the lowest in the entire Iberian Peninsula, i.e. <500 mm or even <300 mm in along most of the coastal area. Precipitation in the watershed feeding the North Catalan margin is always above 600 mm, while in the Cantabrian and Portuguese watersheds opening to the Atlantic Ocean is above 800 mm (AEMET, 2011). Such low particle fluxes in the studied Almeria and Murcia continental margin are also determined by limited shelf to canyon exports due not only to the sediment-starved character of the area but also, and

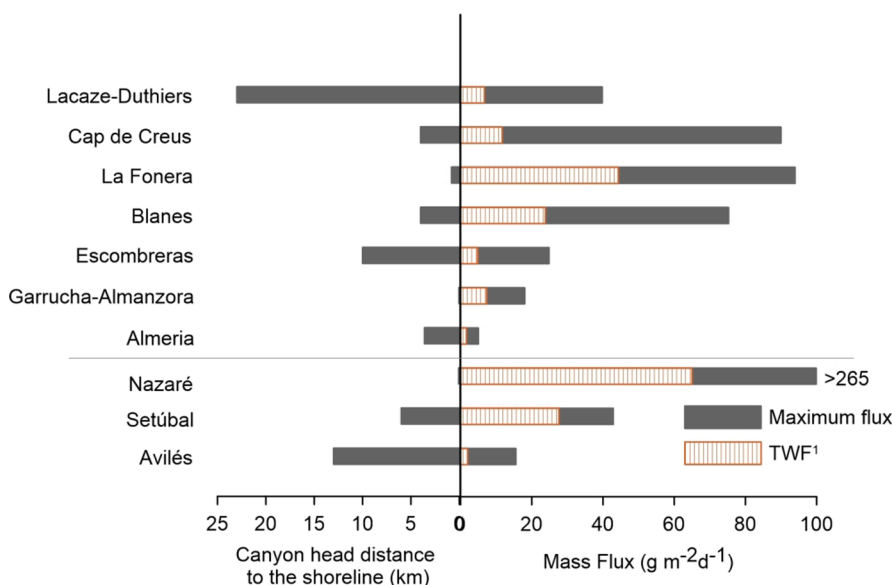


Fig. 11. Shortest canyon head distance to the shoreline (left) and total weighted fluxes (TWF) and maximum TMF (right) in submarine canyons investigated in this study compared to canyons in the NW Mediterranean Sea: Lacaze-Duthiers at 1,000 m depth (Pasqual et al., 2010), Cap de Creus at 1,000 m depth (Pasqual et al., 2010), La Fonera at 1,200 m depth (Martín et al., 2006) Blanes at 1,200 m depth (Lopez-Fernandez et al., 2013b) and in Atlantic Iberian margins: Nazaré at 1,600 m depth (Martín et al., 2011), Setúbal at 1,324 m depth (de Stigter et al., 2011) and Avilés at 2,000 m depth (Rumín-Caparrós et al., 2016). The horizontal line separates Mediterranean canyons (above) from Atlantic canyons (below). Note that the data on Atlantic canyons correspond to larger water depths than Mediterranean canyons. The location of all those canyons is shown in Fig. 1. 1: Mean values of TMF have been used it when the TWF was not available.

importantly, by the mildness of metoceanic conditions during most of the time, with scarce recurrence of extreme events, including major storms. Such events, bringing high amounts of energy to the system, are instead much more frequent in the North Catalan area and even more in Atlantic regions (Martín et al., 2006; Ulses et al., 2008; Martín et al., 2011; Sanchez-Vidal et al., 2012; Rumín-Caparrós et al., 2016). Finally, the lack of high-energy oceanographic processes dominating in and off canyon sediment transport in other margins, such as DSWC, does not help in steering shelf to slope particle export in the investigated margin. However, low recurrence, massive transport events may occur in the study area as triggered by strong earthquakes and rare extreme precipitation and flood events (Sánchez-García et al., 2019).

6. Conclusions

The analysis of the temporal variability and geochemical properties of particle fluxes provides relevant information on sediment dynamics and particle sources in the sediment-starved Almeria and Murcia continental margin and adjacent deep basin. Our results show that storms are the main trigger of mass transfer from the shallow shelf to the deep slope and basin, enhancing particle fluxes both within submarine canyons and in the open slope. In that respect, the magnitude, direction, associated precipitation and duration of the storms eventually leading to high waves and river discharge events, together with the length of intervals between storm events, are the key factors driving down margin mass transfers. A March 2015 to March 2016 year-round monitoring experiment has shown that most particle export to the deep margin occurred as a result of a set of north-east storms in spring 2015 with noticeable wave heights. During that period, off-shelf export of sediment-laden waters was enhanced due to a storm-induced downwelling process. Also, the detachment of turbid layers from the shelf break and the canyons' floor prompted the transport of particle towards deeper reaches. On the other side, the presence of WiW and an associated pycnocline in the Gulf of Vera restricted the vertical particle transfer to a few hundred meters, as illustrated by an above WiW turbid layer at 200 m depth spreading from the outer shelf over the Escombreras mid-canyon reach after a storm in March 2015 in the Mazarron margin segment (Fig. 1).

While metoceanographic processes appear to dominate sedimentary dynamics in Almeria and Escombreras canyons, at the southern and northern ends of the study area, bottom trawling also impacts particle fluxes inside the Garrucha-Almanzora Canyon system in the middle of the study area. Here, the closeness of various canyon heads to river mouths enhances the transfer of terrestrial OC into this system, which should result in an enhanced fertilization of the area making it attractive for the local fishing industry.

Concerning the deep basin traps (mid-water and near-bottom), particle fluxes are mostly determined by phytoplankton blooms. Advective fluxes coming from the continental margin seem to increment TMFs mostly in the near-bottom trap. In any case, the very low fluxes measured in both mid-water and near-bottom traps indicate that few terrestrial particles reach the deep basin in the Gulf of Vera.

Overall, low particle fluxes are recorded in Escombreras, Garrucha-Almanzora and Almeria canyons compared to other canyons in the Western Mediterranean Sea. The lack of recurrent high-energy oceanographic events and the scarcity of riverine sediment inputs are the most relevant factors conditioning the low TMFs observed in the study area. However, longer and complete temporal series are needed to better establish sediment transfer patterns along the Almeria and Murcia continental margin as well to assess inter-annual variability and the likely system shaking effects of rare major storms in the area.

Declaration of Competing Interest

The authors declare that they have no known competing financial interests or personal relationships that could have appeared to influence the work reported in this paper.

Acknowledgements

We would like to express our gratitude to the many colleagues and technicians and to the crew of RV Angeles Alvariño for their dedication and help during sea-going work. We also thank M. Guart for her assistance with laboratory analyses. This work was supported by research projects NUREIEV (ref. CTM2013-44598-R) and NUREIEVA (ref. CTM2016-75953-C2-1-R). GRC Geociències Marines is funded by the

Catalan Government within its excellence research groups program (ref. 2017 SGR 315). M.Tarrés was supported by a FPI grant from *Ministerio de Ciencia, Innovación y Universidades* of the Spanish Government.

References

- Acosta, J., Fontán, A., Muñoz, A., Muñoz-Martín, A., Rivera, J., Uchupi, E., 2013. The morpho-tectonic setting of the Southeast margin of Iberia and the adjacent oceanic Algero-Balearic Basin. *Mar. Pet. Geol.* 45, 17–41. <https://doi.org/10.1016/j.marpetgeo.2013.04.005>.
- AEMET, 2011. Atlas climático ibérico. Temperatura del aire y precipitación (1971-2000). Agencia Estatal de Meteorología, Ministerio de Medio Ambiente y Medio Rural y Marino, e Instituto de Meteorología de Portugal.
- Aemet, 2016. Avance climatológico mensual febrero 2016. Región de Murcia, Agencia Estatal de Meteorología.
- Baker, E.T., Milburn, H.B., Tennant, D.A., 1988. Field assessment of sediment trap efficiency under varying flow conditions. *J. Mar. Res.* 46 (3), 573–592. <https://doi.org/10.1357/002224088785113522>.
- Baldacci, A., Corsini, G., Grasso, R., Manzella, G., Allen, J.T., Cipollini, P., Guymer, T.H., Snaith, H.M., 2001. A study of the Alboran Sea mesoscale system by means of empirical orthogonal function decomposition of satellite data. *J. Mar. Syst.* 29 (1-4), 293–311. [https://doi.org/10.1016/S0924-7963\(01\)00021-5](https://doi.org/10.1016/S0924-7963(01)00021-5).
- Béthoux, J.P., Durrieu de Madron, X., Nyffeler, F., Tailleux, D., 2002. Deep water in the western Mediterranean: peculiar 1999 and 2000 characteristics, shelf formation hypothesis, variability since 1970 and geochemical inferences. *J. Mar. Syst.* 33–34, 117–131. [https://doi.org/10.1016/S0924-7963\(02\)00055-6](https://doi.org/10.1016/S0924-7963(02)00055-6).
- Bonnin, J., Heussner, S., Calafat, A., Fabres, J., Palanques, A., Durrieu de Madron, X., Canals, M., Puig, P., Avril, J., Delsaut, N., 2008. Comparison of horizontal and downward particle fluxes across canyons of the Gulf of Lions (NW Mediterranean): Meteorological and hydrodynamical forcing. *Cont. Shelf Res.* 28 (15), 1957–1970. <https://doi.org/10.1016/j.csr.2008.06.004>.
- Buesseler, K.O., Antia, A.N., Avan, N., Chen, M., Fowler, S.W., Gardner, W.D., Gustafsson, O., Harada, K., Michaels, A.F., Rutgers van der Loeff, M., Sarin, M., Steinberg, D.K., Trull, T., 2007. An assessment of the use of sediment traps for the estimating upper ocean particle fluxes. *J. Mar. Res.* 65, 345–416. <https://doi.org/10.1357/002224007781567621>.
- Canals, M., Company, J.B., Martín, D., Sanchez-Vidal, A., Ramírez-Llorda, E., 2013. Integrated study of Mediterranean deep canyons: novel results and future challenges. *Prog. Oceanogr.* 118, 1–27. <https://doi.org/10.1016/j.pocean.2013.09.004>.
- Canals, M., Puig, P., Durrieu de Madron, X., Heussner, S., Palanques, A., Fabres, J., 2006. Flushing submarine canyons. *Nature* 444 (7117), 354–357. <https://doi.org/10.1038/nature05271>.
- Comas, M.C., Platt, J.P., Soto, J.I., Watts, A.B., 1999. The origin and tectonic history of the Alboran Basin: insights from leg 161 results. *Proc. ODP Sci. Results* 161, 555–580. <https://doi.org/10.2973/odp.proc.ser.161.262.1999>.
- Company, J.B., Puig, P., Sardà, F., Palanques, A., Latasa, M., Scharek, R., Humphries, S., 2008. Climate influence on deep sea populations. *PLoS ONE* 3 (1), e1431. <https://doi.org/10.1371/journal.pone.0001431>.
- Cronin, B.T., Kenyon, N.H., Woodside, J., den Bezemer, T., van der Wal, A., Millington, J., Ivanov, M.K., Limonov, A., 1995. The Almería Canyon: a meandering channel system on an active margin, Alboran Sea, Western Mediterranean. In: Pickering, K. T., Hiscott, R.N., Kenyon, N.H., Ricci-Lucchi, F., Smith, R.D.A. (Eds.), *Atlas of Deep Water Environments: Architectural Style in Turbidite Systems*, 84–88. [Doi: 10.1007/978-94-011-1234-5_15](https://doi.org/10.1007/978-94-011-1234-5_15).
- Drake, D.E., Gorsline, D.S., 1973. Distribution and transport of suspended particulate matter in Hueneme, Redondo, Newport, and La Jolla submarine canyons, California. *Geol. Soc. Am. Bull.* 84, 3949–3968. [https://doi.org/10.1130/0016-7606\(1973\)84<3949:DATOSP>2.0.CO;2](https://doi.org/10.1130/0016-7606(1973)84<3949:DATOSP>2.0.CO;2).
- Dumas, C., Aubert, D., Durrieu de Madron, X., Ludwig, W., Heussner, S., Delsaut, N., Menniti, C., Sotin, C., Buscail, R., 2014. Storm-induced transfer of particulate trace metals to the deep-sea in the Gulf of Lion (NW Mediterranean Sea). *Environ. Geochem. Health* 36 (5), 995–1014. <https://doi.org/10.1007/s10653-014-9614-7>.
- Durrieu de Madron, X., Nyffeler, F., Godet, C.H., 1990. Hydrographic structure and nepheloid spatial distribution in the Gulf of Lions continental margin. *Cont. Shelf Res.* 10 (9–11), 915–929. [https://doi.org/10.1016/0278-4343\(90\)90067-V](https://doi.org/10.1016/0278-4343(90)90067-V).
- Durrieu de Madron, X., Wiberg, P.L., Puig, P., 2008. Sediment dynamics in the Gulf of Lions: the impact of extreme events. *Cont. Shelf Res.* 28 (15), 1867–1876. <https://doi.org/10.1016/j.csr.2008.08.001>.
- Durrieu de Madron, X., Zervakis, V., Theocharis, A., Georgopoulos, D., 2005. Comments on “Cascades of dense water around the world ocean”. *Prog. Oceanogr.* 64 (1), 83–90. <https://doi.org/10.1016/j.pocean.2004.08.004>.
- Estrada, F., Ercilla, G., Alonso, B., 1997. Pliocene-Quaternary tectonic-sedimentary evolution of the NE Alboran Sea (SW Mediterranean Sea). *Tectonophysics* 282 (1-4), 423–442. [https://doi.org/10.1016/S0040-1951\(97\)00227-8](https://doi.org/10.1016/S0040-1951(97)00227-8).
- Estrada, M., Marrasé, C., Latasa, M., Berdalet, E., Delgado, M., Riera, T., 1993. Variability of deep chlorophyll maximum characteristics in the Northwestern Mediterranean. *Mar. Ecol. Prog. Ser.* 92, 289–300. <https://doi.org/10.3354/meps092289>.
- Fabres, J., Calafat, A., Sanchez-Vidal, A., Canals, M., Heussner, S., 2002. Composition and spatio-temporal variability of particle fluxes in the Western Alboran Gyre, Mediterranean Sea (SW Mediterranean). *J. Mar. Syst.* 33–34, 431–456. [https://doi.org/10.1016/S0924-7963\(02\)00070-2](https://doi.org/10.1016/S0924-7963(02)00070-2).
- Fabres, J., Tesi, T., Velez, J., Batista, F., Lee, C., Calafat, A., Heussner, S., Palanques, A., Miserocchi, S., 2008. Seasonal and event-controlled export of organic matter from the shelf towards the Gulf of Lions continental slope. *Cont. Shelf Res.* 28 (15), 1971–1983. <https://doi.org/10.1016/j.csr.2008.04.010>.
- Ferré, B., Guizien, K., Durrieu de Madron, X., Palanques, A., Guillén, J., Grémare, A., 2005. Fine-grained sediment dynamics during a strong storm event in the inner-shelf of the Gulf of Lion (NW Mediterranean). *Cont. Shelf Res.* 25 (19-20), 2410–2427. <https://doi.org/10.1016/j.csr.2005.08.017>.
- García-Gorri, E., Carr, M.-E., 2001. Physical control of phytoplankton distributions in the Alboran Sea: A numerical and satellite approach. *J. Geophys. Res.* 106 (C8), 16795–16805. <https://doi.org/10.1029/1999JC000029>.
- García, M., Alonso, B., Ercilla, G., Gràcia, E., 2006. The tributary valley systems of the Almería Canyon (Alboran Sea, SW Mediterranean): Sedimentary architecture. *Mar. Geol.* 226 (3-4), 207–223. <https://doi.org/10.1016/j.margeo.2005.10.002>.
- García-Rodríguez, M., 2005. La gamba roja “*Aristeus antennatus*” (Risso, 1816) (Crustacea, Decapoda): distribución, demografía, crecimiento, reproducción y explotación en el Golfo de Alicante, Canal de Ibiza y Golfo de Vera. Tesis de la Universidad Complutense de Madrid, Facultad de Ciencias Biológicas. Departamento de Biología Animal I.
- Gardner, W.D., 1985. The effect of tilt on sediment trap efficiency. *Deep-Sea Res.* 32 (3), 349–361. [https://doi.org/10.1016/0198-0149\(85\)90083-4](https://doi.org/10.1016/0198-0149(85)90083-4).
- Gómez de la Peña, L., Gràcia, E., Muñoz, E., Acosta, J., Gómez-Ballesteros, M., Ranero, C. R., Uchupi, E., 2016. Geomorphology and Neogene tectonic evolution of the Palomares continental margin (Western Mediterranean). *Tectonophysics* 689, 25–39. <https://doi.org/10.1016/j.tecto.2016.03.009>.
- Goñi, M.A., Hedges, J.I., 1995. Sources and reactivities of marine derived organic matter in coastal sediments as determined by alkaline CuO oxidation. *Geochim. Cosmochim. Acta* 59, 2965–2981. [https://doi.org/10.1016/0016-7037\(95\)00188-3](https://doi.org/10.1016/0016-7037(95)00188-3).
- Gràcia, E., Pallàs, R., Soto, J.I., Comas, M., Moreno, X., Masana, E., Santanach, P., Díez, S., García, M., Danobeitia, J., 2006. Active faulting offshore SE Spain (Alboran Sea): Implications for earthquake hazard assessment in the Southern Iberian Margin. *Earth Planet. Sci. Lett.* 241 (3-4), 734–749. <https://doi.org/10.1016/j.epsl.2005.11.009>.
- Guillén, J., Bourrin, F., Palanques, A., Durrieu de Madron, X., Puig, P., Buscail, R., 2006. Sediment dynamics during wet and dry storm events on the Têt inner shelf (SW Gulf of Lions). *Mar. Geol.* 234 (1-4), 129–142. <https://doi.org/10.1016/j.margeo.2006.09.018>.
- Hedges, J.I., Keil, R.G., Benner, R., 1997. What happens to terrestrial organic matter in the ocean? *Org. Geochem.* 27 (5-6), 195–212. [https://doi.org/10.1016/S0146-6380\(97\)00066-1](https://doi.org/10.1016/S0146-6380(97)00066-1).
- Hermoso, A., Homar, V., Amengual, A., 2021. The Sequence of Heavy Precipitation and Flash Flooding of 12 and 13 September 2019 in Eastern Spain. Part I: Mesoscale Diagnostic and Sensitivity Analysis of Precipitation. *J. Hydrometeorol.* 22 (5), 1117–1138. <https://doi.org/10.1175/JHM-D-20-0182.1>.
- Hernández-Almeida, I., Bárcena, M.A., Flores, J.A., Siero, F.J., Sanchez-Vidal, A., Calafat, A., 2011. Microplankton response to environmental conditions in the Alboran Sea (Western Mediterranean): One year sediment trap record. *Mar. Micropaleontol.* 78 (1-2), 14–24. <https://doi.org/10.1016/j.marmicro.2010.09.005>.
- Heussner, S.D., de Madron, X., Radakovitch, O., Beaufort, L., Biscaye, P.E., Carbonne, J., Desaut, N., Etcheber, H., Monaco, A., 1999. Spatial and temporal patterns of downward particle fluxes on the continental slope of the Bay of Biscay (northeastern Atlantic). *Deep-Sea Res.* II 46, 2101–2146. [https://doi.org/10.1016/S0967-0645\(99\)00057-0](https://doi.org/10.1016/S0967-0645(99)00057-0).
- Heussner, S., Durrieu de Madron, X., Calafat, A., Canals, M., Carbonne, J., Delsaut, N., Saragoni, G., 2006. Spatial and temporal variability of downward particle fluxes on a continental slope: lessons from an 8-yr experiment in the Gulf of Lions (NW Mediterranean). *Mar. Geol.* 234 (1-4), 63–92. <https://doi.org/10.1016/j.margeo.2006.09.003>.
- Heussner, S., Ratti, C., Carbonne, J., 1990. The PPS 3 time-series sediment trap and the trap sample processing techniques used during the ECOMARGE experiment. *Cont. Shelf Res.* 10 (9-11), 943–958. [https://doi.org/10.1016/0278-4343\(90\)90069-X](https://doi.org/10.1016/0278-4343(90)90069-X).
- Juza, M., Escudier, R., Vargas-Yáñez, M., Mourre, B., Heslop, E., Allen, J., Tintoré, J., 2019. Characterization of changes in Western Intermediate Water properties enabled by an innovative geometry-based detection approach. *J. Mar. Syst.* 191, 1–12. <https://doi.org/10.1016/j.jmarsys.2018.11.003>.
- Kamatani, A., Oku, O., 2000. Measuring biogenic silica in marine sediments. *Mar. Chem.* 68 (3), 219–229. [https://doi.org/10.1016/S0304-4203\(99\)00079-1](https://doi.org/10.1016/S0304-4203(99)00079-1).
- Kiriakoulakis, K., Blackburn, S., Ingels, J., Vanreusel, A., Wolff, G.A., 2011. Organic geochemistry of submarine canyons: The Portuguese Margin. *Deep-Sea Res.* II 58 (23-24), 2477–2488. <https://doi.org/10.1016/j.dsr2.2011.04.010>.
- Langone, L., Conese, I., Miserocchi, S., Boldrin, A., Bonaldo, D., Carniel, S., Chiggiato, J., Turchetto, M., Borghini, M., Tesi, T., 2016. Dynamics of particles along the western margin of the Southern Adriatic: Processes involved in transferring particulate matter to the deep basin. *Mar. Geol.* 375, 28–43. <https://doi.org/10.1016/j.margeo.2015.09.004>.
- Liquete, C., Arnau, P., Canals, M., Colas, S., 2005. Mediterranean river systems of Andalusia, southern Spain, and associated deltas: A source to sink approach. *Mar. Geol.* 222–223, 471–495. <https://doi.org/10.1016/j.margeo.2005.06.033>.
- Lobo, F.J., Ercilla, G., Fernández-Salas, L.M., Gámez, D., 2014. Chapter 11 The Iberian Mediterranean shelves. *Geological Society, London, Memoirs* 41 (1), 147–170.
- Lopez-Fernandez, P., Bianchelli, S., Pusceddu, A., Calafat, A., Danovaro, R., Canals, M., 2013a. Bioavailable compounds in sinking particulate organic matter, Blanes Canyon, NW Mediterranean Sea: Effects of a large storm and sea surface biological processes. *Prog. Oceanogr.* 118, 108–121. <https://doi.org/10.1016/j.pocean.2013.07.022>.
- Lopez-Fernandez, P., Calafat, A., Sanchez-Vidal, A., Canals, M., Flexas, M.M., Cateura, J., Company, J.B., 2013b. Multiple drivers of particle fluxes in the Blanes submarine

- canyon and adjacent open slope: results of a year round experiment. *Prog. Oceanogr.* 118, 95–107. <https://doi.org/10.1016/j.pocean.2013.07.029>.
- Machado, M.J., Benito, G., Barriendos, M., Rodrigo, F.S., 2011. 500 years of rainfall variability and extreme hydrological events in southeastern Spain drylands. *J. Arid Environ.* 75 (12), 1244–1253. <https://doi.org/10.1016/j.jaridenv.2011.02.002>.
- Martín, J., Durrieu de Madron, X., Puig, P., Bourrin, F., Palanques, A., Houpert, L., Higuera, M., Sanchez-Vidal, A., Calafat, A.M., Canals, M., Heussner, S., Desaut, N., Sotin, C., 2013. Sediment transport along the Cap de Creus Canyon flank during a mild, wet winter. *Biogeosciences* 10, 3221–3239. <https://doi.org/10.5194/bg-10-3221-2013>.
- Martín, J., Palanques, A., Puig, P., 2006. Composition and variability of downward particulate matter fluxes in the Palamós submarine canyon (NW Mediterranean). *J. Mar. Syst.* 60 (1–2), 75–97. <https://doi.org/10.1016/j.jmarsys.2005.09.010>.
- Martín, J., Palanques, A., Vitorino, J., Oliveira, A., de Stigter, H.C., 2011. Near-bottom particulate matter dynamics in the Nazaré submarine canyon under calm and stormy conditions. *Deep-Sea Res. II* 58 (23–24), 2388–2400. <https://doi.org/10.1016/j.dsr2.2011.04.004>.
- Martín, J., Puig, P., Masqué, P., Palanques, A., Sánchez-Gómez, A., Vopel, K.C., 2014a. Impact of bottom trawling on deep-sea sediment properties along the flanks of a submarine canyon. *PLoS ONE* 9 (8), e104536. <https://doi.org/10.1371/journal.pone.0104536>.
- Martín, J., Puig, P., Palanques, A., Ribó, M., 2014b. Trawling-induced daily sediment resuspension in the flank of a Mediterranean submarine canyon. *Deep-Sea Res. II* 104, 174–183. <https://doi.org/10.1016/j.dsr2.2013.05.036>.
- Masqué, P., Fabres, J., Canals, M., Sanchez-Cabeza, J.A., Sanchez-Vidal, A., Cacho, I., Calafat, A.M., Bruach, J.M., 2003. Accumulation rates of major constituents of hemipelagic sediments in the deep Alboran Sea: A centennial perspective of sedimentary dynamics. *Mar. Geol.* 193 (3–4), 207–233. [https://doi.org/10.1016/S0025-3227\(02\)00593-5](https://doi.org/10.1016/S0025-3227(02)00593-5).
- Millot, C., 1999. Circulation in the Western Mediterranean Sea. *J. Mar. Syst.* 20 (1–4), 423–442. [https://doi.org/10.1016/S0924-7963\(98\)00078-5](https://doi.org/10.1016/S0924-7963(98)00078-5).
- Mortlock, R.A., Froelich, P.N., 1989. A simple method for the rapid determinations of biogenic opal in pelagic marine sediments. *Deep-Sea Res.* 36 (9), 1415–1426. [https://doi.org/10.1016/0198-0149\(89\)90092-7](https://doi.org/10.1016/0198-0149(89)90092-7).
- Muñoz, M., Reul, A., García-Martínez, M.C., Plaza, F., Bautista, B., Moya, F., Vargas-Yáñez, M., 2018. Oceanographic and bathymetric features as the target for pelagic MPA design: A case study on the Cape of Gata. *Water* 10, 1403. <https://doi.org/10.3390/w10101403>.
- Ogston, A.S., Drexler, T.M., Puig, P., 2008. Sediment delivery, resuspension, and transport in two contrasting canyon environments in the southwest Gulf of Lions. *Cont. Shelf Res.* 28 (15), 2000–2016. <https://doi.org/10.1016/j.csr.2008.02.012>.
- Palanques, A., Durrieu de Madron, X., Puig, P., Fabres, J., Guillén, J., Calafat, A., Canals, M., Heussner, S., Bonnín, J., 2006a. Suspended sediment fluxes and transport processes in the Gulf of Lions submarine canyons. The role of storms and dense water cascading. *Mar. Geol.* 234 (1–4), 43–61. <https://doi.org/10.1016/j.margeo.2006.09.002>.
- Palanques, A., El Khatib, M., Puig, P., Masqué, P., Sánchez-Cabeza, J.A., Isla, E., 2005. Downward particle fluxes in the Guadiaro submarine canyon depositional system (north-western Alboran Sea), a river flood dominated system. *Mar. Geol.* 220 (1–4), 23–40. <https://doi.org/10.1016/j.margeo.2005.07.004>.
- Palanques, A., Guillén, J., Puig, P., Durrieu de Madron, X., 2008a. Storm-driven shelf-to-canyon suspended sediment transport at the southwestern Gulf of Lions. *Cont. Shelf Res.* 28 (15), 1947–1956. <https://doi.org/10.1016/j.csr.2008.03.020>.
- Palanques, A., Martín, J., Puig, P., Guillén, J., Company, J.B., Sardà, F., 2006b. Evidence of sediment gravity flows induced by trawling in the Palamós (Fonera) submarine canyon (northwestern Mediterranean). *Deep-Sea Res. I* 53 (2), 201–214. <https://doi.org/10.1016/j.dsr.2005.10.003>.
- Palanques, A., Masqué, P., Puig, P., Sanchez-Cabeza, J.A., Frignani, M., Alvisi, F., 2008b. Anthropogenic trace metals in the sedimentary record of the Llobregat continental shelf and adjacent Foix Submarine Canyon (northwestern Mediterranean). *Mar. Geol.* 248 (3–4), 213–227. <https://doi.org/10.1016/j.margeo.2007.11.001>.
- Palanques, A., Puig, P., Durrieu de Madron, X., Sanchez-Vidal, A., Pasqual, C., Martín, J., Calafat, A., Heussner, S., Canals, M., 2012. Sediment transport to the deep canyons and open-slope of the western Gulf of Lions during the 2006 intense cascading and open-sea convection period. *Prog. Oceanogr.* 106, 1–15. <https://doi.org/10.1016/j.pocean.2012.05.002>.
- Paradis, S., Puig, P., Masqué, P., Juan-Díaz, X., Martín, J., Palanques, A., 2017. Bottom-trawling along submarine canyons impacts deep sedimentary regimes. *Sci. Rep.* 7, 43332. <https://doi.org/10.1038/srep43332>.
- Pasqual, C., Sanchez-Vidal, A., Zuñiga, D., Calafat, A., Canals, M., Durrieu de Madron, X., Puig, P., Heussner, S., Palanques, A., Delsaut, N., 2010. Flux and composition of settling particles across the continental margin of the Gulf of Lion: the role of dense shelf water cascading. *Biogeosciences* 7, 217–231. <https://doi.org/10.5194/bg-7-217-2010>.
- Payo-Payo, M., Jacinto, R.S., Lastras, G., Rabineau, M., Puig, P., Martín, J., Canals, M., Sultan, N., 2017. Numerical modeling of bottom trawling-induced sediment transport and accumulation in La Fonera submarine canyon, northwestern Mediterranean Sea. *Mar. Geol.* 386, 107–125. <https://doi.org/10.1016/j.margeo.2017.02.015>.
- Pedrosa-Pàmies, R., Sanchez-Vidal, A., Calafat, A., Canals, M., Durán, R., 2013. Impact of storm-induced remobilization on grain size distribution and organic carbon content in sediments from the Blanes Canyon area, NW Mediterranean Sea. *Prog. Oceanogr.* 118, 122–136. <https://doi.org/10.1016/j.pocean.2013.07.023>.
- Pérez-Hernández, S., Comas, M.C., Escutia, C., 2014. Morphology of turbidite systems within an active continental margin (the Palomares Margin, western Mediterranean). *Geomorphology* 219, 10–26. <https://doi.org/10.1016/j.geomorph.2014.04.014>.
- Puig, P., Canals, M., Company, J.B., Martín, J., Amblas, D., Lastras, G., Palanques, A., Calafat, A.M., 2012. Ploughing the deep sea floor. *Nature* 489 (7415), 286–289. <https://doi.org/10.1038/nature11410>.
- Puig, P., Durán, R., Muñoz, A., Elvira, E., Guillén, J., 2017. Submarine canyon-head morphologies and inferred sediment transport processes in the Alías-Almanzora canyon system (SW Mediterranean): On the role of the sediment supply. *Mar. Geol.* 393, 21–34. <https://doi.org/10.1016/j.margeo.2017.02.009>.
- Puig, P., Palanques, A., Guillén, J., El Khatib, M., 2004. Role of internal waves in the generation of nepheloid layers on the northwestern Alboran slope: implications for continental margin shaping. *J. Geophys. Res.* 109, C09011. <https://doi.org/10.1029/2004JC002394>.
- Puig, P., Palanques, A., Martín, J., 2014. Contemporary Sediment-Transport Processes in Submarine Canyons. *Ann. Rev. Mar. Sci.* 6 (1), 53–77. <https://doi.org/10.1146/annurev-marine-010213-135037>.
- Puscaddu, A., Mea, M., Canals, M., Heussner, S., Durrieu de Madron, X., Sanchez-Vidal, A., Bianchelli, S., Corinaldesi, C., Dell'Anno, A., Thomsen, L., Danovaro, R., 2013. Major consequences of an intense dense shelf water cascading event on deep-sea benthic trophic conditions and meiofaunal biodiversity. *Biogeosciences* 10 (4), 2659–2670. <https://doi.org/10.5194/bg-10-2659-2013>. <https://doi.org/10.5194/bg-10-2659-2013-supplement>.
- Ramírez-Llodra, E., De Mol, B., Company, J.B., Coll, M., Sardà, F., 2013. Effects of natural and anthropogenic processes in the distribution of marine litter in the deep Mediterranean Sea. *Prog. Oceanogr.* 118, 273–287. <https://doi.org/10.1016/j.pocean.2013.07.027>.
- Renault, L., Oguz, T., Pascual, A., Vizoso, G., Tintore, J., 2012. Surface circulation in the Alboran Sea (western Mediterranean) inferred from remotely sensed data. *J. Geophys. Res.* 117, C08009. <https://doi.org/10.1029/2011JC007659>.
- Romero-Romero, S., Molina-Ramírez, A., Höfer, J., Duineveld, G., Rumín-Caparrós, A., Sanchez-Vidal, A., Canals, M., Acuña, J.L., 2016. Seasonal pathways of organic matter within the Avilés submarine canyon: Food web implications. *Deep Sea Res. Part I* 117, 1–10. <https://doi.org/10.1016/j.dsr.2016.09.003>.
- Rumín-Caparrós, A., Sanchez-Vidal, A., González-Pola, C., Lastras, G., Calafat, A., Canals, M., 2016. Particle fluxes and their drivers in the Avilés submarine canyon and adjacent slope, central Cantabrian margin, Bay of Biscay. *Prog. Oceanogr.* 144, 39–61. <https://doi.org/10.1016/j.pocean.2016.03.004>.
- Sánchez-García, C., Schulte, L., Carvalho, F., Peña, J.C., 2019. A 500-year flood history of the arid environments of southeastern Spain. The case of the Almanzora River. *Global Planet. Change* 181, 102987. <https://doi.org/10.1016/j.gloplacha.2019.102987>.
- Sanchez-Vidal, A., Canals, M., Calafat, A.M., Lastras, G., Pedrosa-Pàmies, R., Menéndez, M., Medina, R., Company, J.B., Hereu, B., Romero, J., Alcoverro, T., Chin, W.-C., 2012. Impacts on the deep-sea ecosystem by a severe coastal storm. *PLoS ONE* 7 (1), e30395. <https://doi.org/10.1371/journal.pone.0030395>.
- Sanchez-Vidal, A., Higuera, M., Martí, E., Liqueur, C., Calafat, A., Kerhervé, P., Canals, M., 2013. Riverine transport of terrestrial organic matter to the North Catalan margin, NW Mediterranean Sea. *Prog. Oceanogr.* 118, 71–80. <https://doi.org/10.1016/j.pocean.2013.07.020>.
- Sanchez-Vidal, A., Calafat, A., Canals, M., Frigola, J., Fabres, J., 2005. Particle fluxes and organic carbon balance across the Eastern Alboran Sea (SW Mediterranean Sea). *Cont. Shelf Res.* 25 (5–6), 609–628. <https://doi.org/10.1016/j.csr.2004.11.004>.
- Sanz, J.L., Hermida, N., Lobato, A.B., Tello, O., Fernández-Salas, L.M., González, J.L., Bécares, M.A., Gómez de Paz, R., Cubero, P., González, F., Muñoz, A., Vaquero, M., Ubiedo, J.M., Contreras, D., Ramos, M., Carreño, F., Pérez, J.I., 2002. Estudio de la Plataforma Continental Española, Hoja MC047-Garrucha-Serie C. Secretaría General de Pesca Marítima e Instituto Español de Oceanografía.
- Sarhan, T., García Lafuente, J., Vargas, M., Vargas, J.M., Plaza, F., 2000. Upwelling mechanisms in the northwestern Alboran Sea. *J. Marine Syst.* 23, 317–331. [https://doi.org/10.1016/S0924-7963\(99\)00068-8](https://doi.org/10.1016/S0924-7963(99)00068-8).
- Schmidt, S., de Stigter, H.C., van Weering, T.C.E., 2001. Enhanced short-term sediment deposition within the Nazaré Canyon, North-East Atlantic. *Marine Geol.* 173 (1–4), 55–67. [https://doi.org/10.1016/S0025-3227\(00\)00163-8](https://doi.org/10.1016/S0025-3227(00)00163-8).
- Schmidt, S., Howa, H., Diallo, A., Martín, J., Cremer, M., Duros, P., Fontanier, C., Deflandre, B., Metzger, E., Mulder, T., 2014. Recent sediment transport and deposition in the Cap-Ferret Canyon, South-East margin of Bay of Biscay. *Deep-Sea Res. II* 104, 134–144. <https://doi.org/10.1016/j.dsr2.2013.06.004>.
- Shepard, F.P., Marshall, N.F., McLoughlin, P.A., Sullivan, G.G., 1979. Currents in Submarine Canyons and Other Seamounts. AAPG Studies in Geology 8, Tulsa, Oklahoma, 173. Doi: 10.2110/pec.79.27.0085.
- de Stigter, H.C., Boer, W., de Jesus Mendes, P.A., Jesus, C.C., Thomsen, L., van den Bergh, G.D., van Weering, T.C.E., 2007. Recent sediment transport and deposition in

- the Nazaré Canyon, Portuguese continental margin. *Marine Geol.* 246 (2–4), 144–164. <https://doi.org/10.1016/j.margeo.2007.04.011>.
- de Stigter, H.C., Jesus, C.C., Boer, W., Richter, T.O., Costa, A., van Weering, T.C.E., 2011. Recent sediment transport and deposition in the Lisbon-Setúbal and Cascais submarine canyons. Portuguese continental margin. *Deep-Sea Res. II* 58 (23–24), 2321–2344. <https://doi.org/10.1016/j.dsr2.2011.04.001>.
- Tintore, J., La Violette, P.E., Blade, I., Cruzado, A., 1988. A study of an intense density front in the Eastern Alboran Sea: the Almeria-Oran Front. *J. Phys. Oceanogr.* 18, 1384–1397. [https://doi.org/10.1175/1520-0485\(1988\)018<1384:ASOAIID>2.0.CO;2](https://doi.org/10.1175/1520-0485(1988)018<1384:ASOAIID>2.0.CO;2).
- Tubau, X., Canal, M., Lastras, G., Rayo, X., Rivera, J., Amblas, D., 2015. Marine litter on the floor of deep submarine canyons of the Northwestern Mediterranean Sea: The role of hydrodynamic processes. *Prog. Oceanogr.* 134, 379–403. <https://doi.org/10.1016/j.pocean.2015.03.013>.
- Ulses, C., Estournel, C., Durrieu de Madron, X., Palanques, A., 2008. Suspended sediment transport in the Gulf of Lions (NW Mediterranean): impact of extreme storms and floods. *Cont. Shelf Res.* 28 (15), 2048–2070. <https://doi.org/10.1016/j.csr.2008.01.015>.
- Vargas-Yáñez, M., Plaza, F., García-Lafuente, J., Sarhan, T., Vargas, J.M., Vélez-Belchi, P., 2002. About the seasonal variability of the Alboran Sea circulation. *J. Mar. Syst.* 35 (3–4), 229–248. [https://doi.org/10.1016/S0924-7963\(02\)00128-8](https://doi.org/10.1016/S0924-7963(02)00128-8).
- Vargas-Yáñez, M., García-Martínez, M.C., Moya, F., Balbín, R., López-Jurado, J.L., Serra, M., Zunino, P., Pascual, J., Salat, J., 2017. Updating temperature and salinity mean values and trends in the Western Mediterranean: The RADMED Project. *Prog. Oceanogr.* 157, 27–46. <https://doi.org/10.1016/j.pocean.2017.09.004>.
- Vázquez, J.T., Ercilla, G., Alonso, B., Juan, C., Rueda, J.L., Palomino, D., Fernández-Salas, L.M., Bárcenas, P., Casas, D., Díaz-del-Río, V., Estrada, F., Farran, M., García, M., González, E., López-Gonzalez, N., El Mounni, B., and Contouriber, Montera and Mower Teams, 2015. Submarine Canyons and related features in the Alboran Sea: continental margins and major isolated reliefs. pp. 183–196 In *CIESM Monograph 47* [F. Briand ed.] Submarine canyon dynamics in the Mediterranean and tributary seas—An integrated geological, oceanographic and biological perspective, 232 p. CIESM Publisher, Monaco.
- Xu, J.P., Noble, M.A., Rosenfeld, L.K., 2004. In-situ measurements of velocity structure within turbidity currents. *L09311 Geophys. Res. Lett.* 31 (9). <https://doi.org/10.1029/2004GL019718>.
- www.puertos.es/es-es/oceanografia/Paginas/portus.aspx: Puertos del Estado webpage. From which metoceanographic data have been downloaded.